NOAA Technical Memorandum ERL PMEL-45

# WINTER CURRENTS ON THE EASTERN BERING SEA SHELF

Sigrid A. Salo
James D. Schumacher
Lawrence K. Coachman

Pacific Marine Environmental Laboratory
Seattle, Washington
April 1983


UNITED STATES
DEPARTMENT OF COMMERCE
Malcolm Baldrige,
Secretary

NATIONAL OCEANIC AND
ATMOSPHERIC ADMINISTRATION
John V. Byrne,
Administrator

Environmental Research
Laboratories
George H. Ludwig
Director

## NOTICE

Mention of a commercial company or product does not constitute an endorsement by NOAA Environmental Research Laboratories. Use for publicity or advertising purposes of information from this publication concerning proprietary products or the tests of such products is not authorized.

CONTENTS

## FIGURES

## TABLES

# WINTER CURRENTS ON THE EASTERN BERING SEA SHELF[1]

Sigrid A. Salo[2], James E. Schumacher[3], L. K. Coachman[4]

ABSTRACT. An analysis of fifteen current records from thirteen locations over the central and northern Bering Sea shelf is presented. Four moorings were deployed over the 1976/77 and 1977/78 winters and five over winter 1980/81. Comparison of current and kinetic energy characteristics showed a difference between records from north and south of St. Lawrence Island. To the north, circulation was dominated by northward mean flow (4-15 cm/s), and tides accounted for only 24±13% of the total kinetic energy of fluctuations. In contrast, mean currents south of St. Lawrence Island exhibited greater variation in direction, were generally 1 to 4 cm/s in magnitude and tides accounted for about 55±31% of the fluctuating kinetic energy. Although vector-mean currents in both regions were in general northward, and approximately parallel to local bathymetry, frequent reversals occurred. One reversal, coincident with northerly winds, occurred at all sites and persisted for more than two weeks; such current reversals affect the flow over thousands of square kilometers. The presence of ice appears to affect the flow by reducing the impact of direct wind stress as driving force.

---

[1] Contribution No. 605 from the NOAA/ERL Pacific Marine Environmental Laboratory, 3711 15th Avenue N.E., Seattle, Washington 98105.

[2] Present affiliation: Institut de Miveka, B.P. 27, Miveka, Kasai Occidental, Zaire (Zaire Desk, Peace Corps).
Former affiliation: Marine Meteorological Studies Group, PMEL, and School of Oceanography, University of Washington, Seattle, Washington 98195.

[3] Coastal Physics Group, PMEL.

[4] School of Oceanography, University of Washington, Seattle, Washington 98195.

## 1. Introduction

Between 1976 and 1981, the Pacific Marine Environmental Laboratory and University of Washington cooperated in studies of the northern Bering Sea shelf in support of the Outer Continental Shelf Environmental Assessment Program. One facet of this program was the collection of current records from instruments mooring throughout the period of ice cover (Table 1, Figure 1). This report provides a description of tidal and low-frequency currents during winter over the northern Bering Sea shelf from these records. The current data are characterized using rotary spectra, statistical parameters of mean currents, and time series comparisons. The wind field characteristics and their relation to the currents are also examined, using similar methods.

## 2. Background and Oceanographic Setting

North of St. Lawrence Island, the Bering Sea shelf is bounded by the Alaska mainland, Siberia, and the island itself (Fig. 2). Adjoining the northern Bering Sea shelf are three straits: Anadyr Strait and Shpanberg Strait are west and east of St. Lawrence Island, and Bering Strait lies about 250 km to the north. The cross section of these straits are 75 km by 40 m, 200 km by 25 m, and 85 km by 50 m, respectively. The boundary between this shelf region and Norton Sound proper can be placed at the 20-m isobath. The shelf deepens toward the northwest, attaining maximum depths of 50 to 60 m in the vicinity of the Bering Strait.

Horizontal scales on the shelf south of St. Lawrence are much greater. The shelf break lies 750 km southwest of the St. Lawrence Island and 650 km west from the Nunivak Island. The eastern section of this region is less than 50 m deep, and isobaths trend toward the northwest. The depths and local trend of bathymetry for each current meter site, in the northern region and on the open shelf, are listed in Table 1.

Major sources of freshwater to the eastern shelf include the Kuskokwim, Koyukuk, and Kvichak Rivers near Bristol Bay, and the Yukon River north of Cape Romanzof. The Anadyr River is the only large river supplying freshwater to the Gulf of Anadyr and the western shelf. River discharge is seasonal, with peak flow on the eastern shelf occurring in June; Yukon River discharge is then about 15,000 $m^3/s$, or $\sim$1/3 of the total (Coachman et al., 1975). Winter discharge is lower by nearly an order of magnitude, although runoff in September is still greater than 8000 $m^3/s$ (Overland, 1981).

Stratification due to freshwater and insolation exists during summer over much of the study area. By winter, wind-induced mixing in concert with decreased river discharge and latent and sensible heat losses from the surface produce homogeneous water columns. Newton and Anderson (1980) report that at forty percent of CTD stations taken within the ice pack, water columns were vertically well mixed in salinity, and nearly all temperatures were near the freezing point.

Table 1. Background information for each mooring in the data set. Moorings containing two meters are marked with an * and the depths and last record of each meter are given. Ice cover refers to the date following which the site was ice-covered. Ice cover was continuous from freeze-up through March at all meters.

| Mooring | Depth (instrument/water) | Bathym. axis (°T) | Lat. (°N) | Long. (°W) | Deployed (JD) | Last Record (JD) | Ice Cover (JD) |
|---|---|---|---|---|---|---|---|
| NC-10 | 45/55 | 005 | 65.75 | 168.45 | 76235 | 77095 | 76306 |
| NC-14 | 21/32 | 095 | 64.36 | 165.36 | 76234 | 77176 | 76299 |
| NC-17A | 22/24 | 000 | 62.80 | 167.45 | 76245 | 77136 | 76329 |
| NC-16 | 19/29 | 005 | 62.62 | 166.89 | 76272 | 77092 | 76329 |
| NC-23A | 16/26 | 345 | 63.95 | 166.16 | 77264 | 78193 | 77312 |
| NC-17B | 17/26 | 355 | 62.89 | 167.08 | 77263 | 78194 | 77312 |
| *NC-24A | 24,40/48 | 335 | 61.81 | 170.44 | 77262 | 78202(78107) | 77340 |
| *BC-20A | 22,52/66 | 340 | 60.43 | 171.09 | 77260 | 78072(78048) | 77348 |
| BC-21A | | | 60.39 | 169.19 | 77261 | 78342 | 77347 |
| NC-19B | 45/55 | 045 | 63.97 | 172.02 | 80317 | 81180 | 80325 |
| NC-26 | 57/67 | 010 | 63.18 | 173.14 | 80317 | 81180 | 80330 |
| NC-25 | 36/46 | 310 | 63.01 | 170.97 | 80317 | 81180 | 80330 |
| BC-26 | 50/119 | 335 | 60.57 | 176.04 | 80318 | 81155 | 80358 |
| BC-22 | 50/76 | 335 | 59.31 | 171.19 | 80315 | 81156 | 81006 |

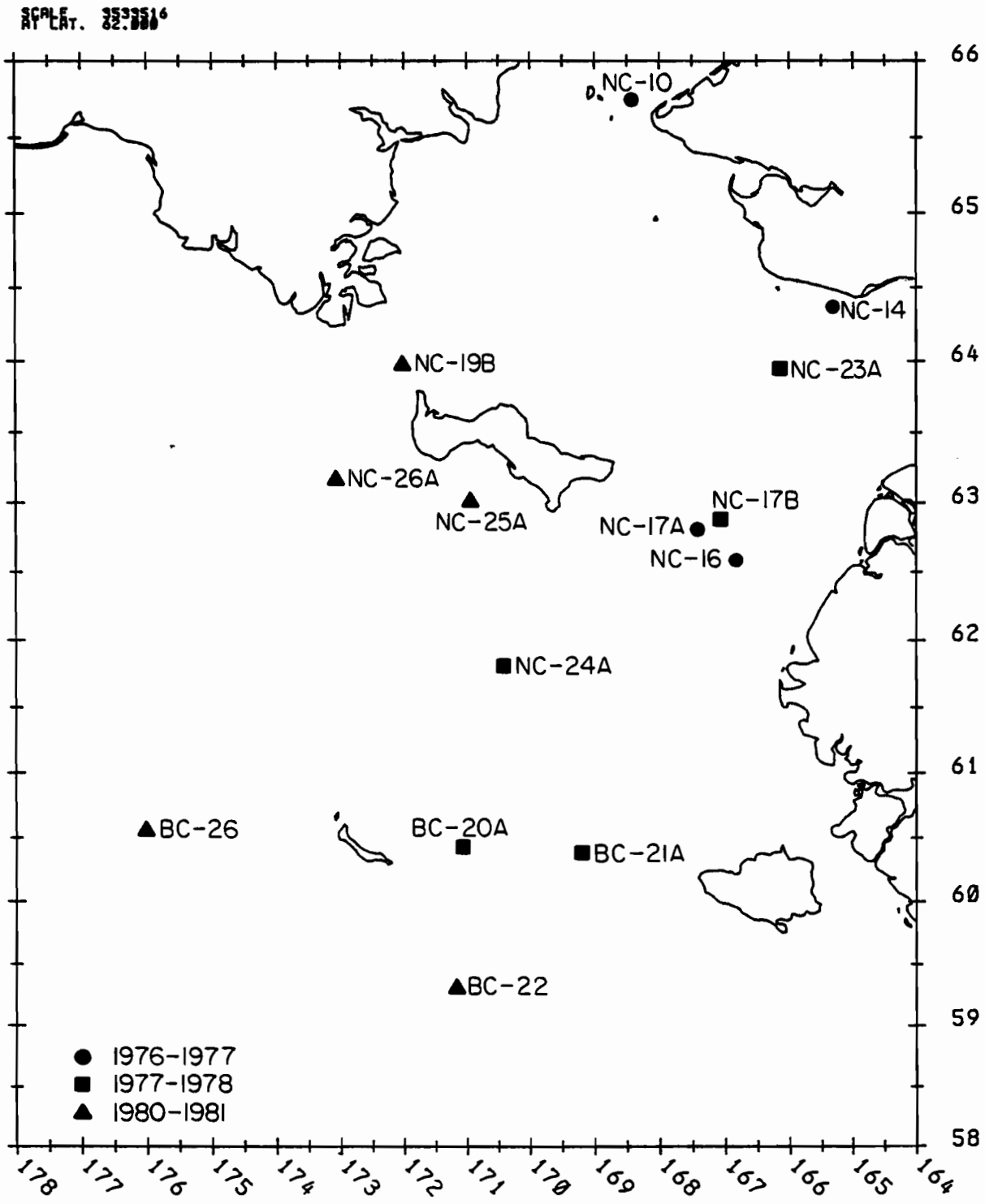


Figure 1. Locations of moorings discussed in this paper.

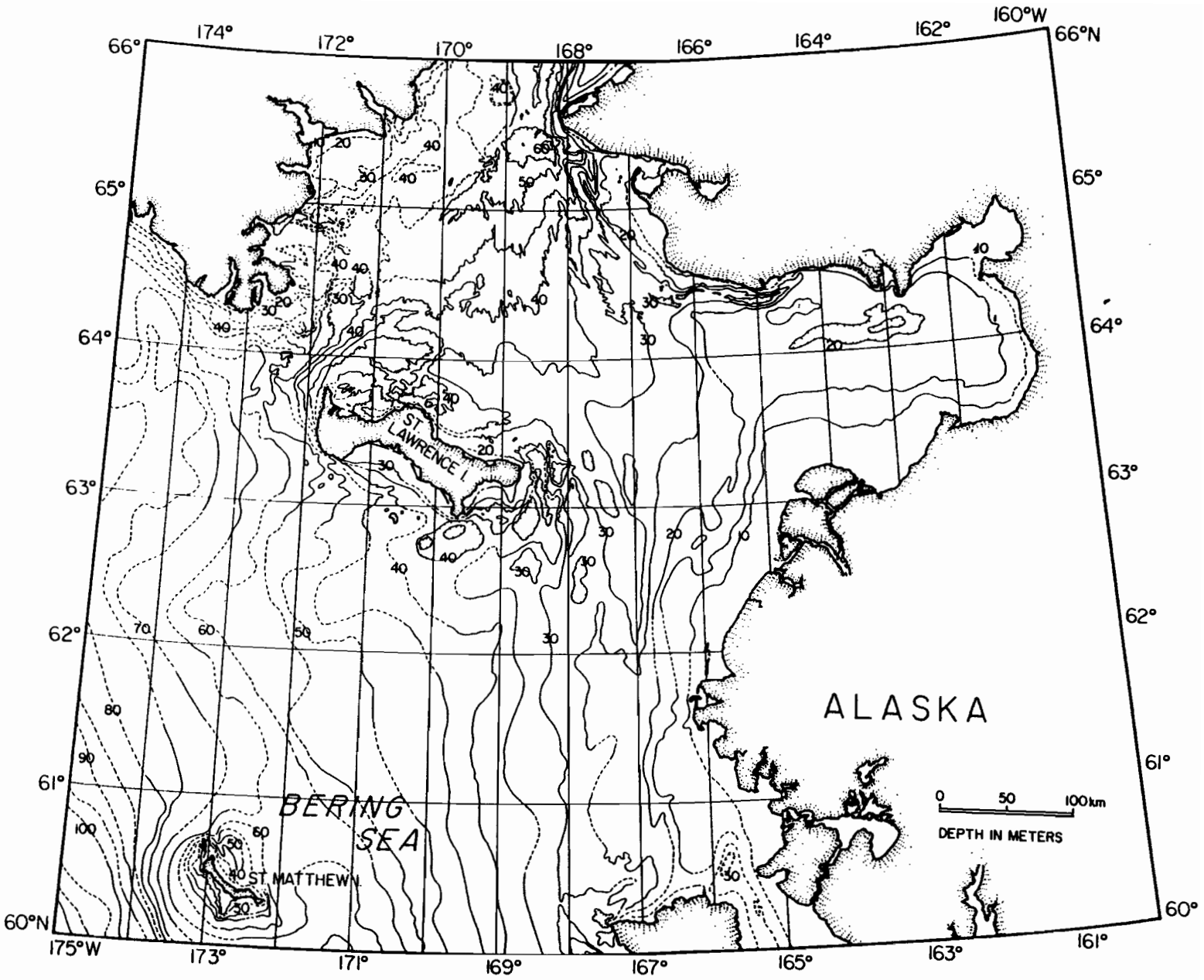


Figure 2. Bathymetry of the central and northern Bering Sea shelf.

Many of the remaining stations were only weakly stratified, with the most pronounced stratification occurring either near the ice edge or in the polynya south of St. Lawrence Island. Stratification near the ice edge is the result of the formation of a layer of cold, fresh meltwater (Pease, 1980; Salo et al., 1980), while that in the polynya results from salinization of deeper water occurring during ice formation.

Webster (1981) shows that by January the 50% probability ice edge is south of the region discussed in this paper. As a first approximation, most ice forms in the Bering Sea at polynyas along the south edge of east-west trending coasts and north wind conditions result in advection southward (Pease, 1981). The contribution of regional currents to this process has not been elucidated, primarily due to the lack of data.

The average atmospheric surface pressure pattern for winter illustrated in Pease et al. (1982) depicts isobars which trend ENE to WSW with higher pressure to the north. This pattern would produce vector-mean surface winds from the northeast. Cyclonic storms are common in the southern Bering Sea during the winter months though they penetrate less frequently into the northern section.

There has been little work published on currents of the central and northern Bering Sea shelf. Even fewer authors discuss winter characteristics of the currents. The primary sources from which the following summary is drawn are a collection of papers edited by D. H. Hood and J. A. Calder (1981) entitled *The Eastern Bering Sea Shelf: Oceanography and Resources (vol. 1)*, and *Bering Strait: The Regional Physical Oceanography* by L. K. Coachman, K. Aagaard, and R. B. Tripp (1975).

Long-term vector-mean flow is directed to the north in nearly all regions of the central and northern Bering Sea shelf. Takenouti and Ohtani (1974) presented a synopsis of circulation based on water mass analysis in the area. In their diagram, currents at the shelf break are toward the northwest, parallel to the bathymetry. The current moves northward into the Gulf of Anadyr, then eastward where it splits. Part continues to flow eastward just south of St. Lawrence Island, while the other part flows northward through the Anadyr Strait. North of St. Lawrence Island, all flow is directed to the north. They do not describe the currents on the eastern shelf between St. Lawrence and Nunivak Islands, nor do they provide estimates of current speeds.

Coachman and Aagaard (1981) estimated from observations a mean annual transport of 0.8 Sv north through Bering Strait. They noted that the northerly direction is a consequence of a mean sea surface slope downward toward the north. Frequent reversals, from northerly to southerly flow, occurred in the current records collected in the Bering Strait area in 1976/77. The apparent cause of the southerly flow events was the removal of water from the Bering Sea shelf south of the St. Lawrence Island by northerly winds. This created a temporary regional sea surface slope downward toward the south, which, in combination with the winds themselves, drove flow to the south.

In the Bering Strait there were considerable variations in currents over short cross-channel distances. Two surveys of currents in Shpanberg Strait also exhibited large cross-channel variations. The transects were taken during July 1968 and September 1976. Flow was to the north in the eastern part of both straits, but currents were southerly in their western parts. Similar horizontal shears in the flow field probably occur in other regions such as the Anadyr Strait.

The north-trending mean current which prevails across the mouth of Norton Sound may at times penetrate more deeply into the sound. In general, wind events were very important to the flow in Norton Sound (Muench et al., 1981).

On the shelf to the southwest of St. Lawrence Island, there was a region of anomalously cold water in summer. This feature could not be maintained if there were substantial flow through the cold spot (Coachman et al., 1975).

Kinder and Schumacher (1981) show that the southeastern Bering Sea shelf can be divided into three flow regimes. Water less than 50 m deep is the coastal regime, which is characterized, in the vicinity of Nunivak Island, by currents with a vector-mean speed of 2-5 cm/s toward the northwest. Within the middle shelf regime (water depths from about 50 to 100 m), mean flow is generally less than 1 cm/s and there is not a characteristic vector-mean direction. The outer shelf regime lies between the 100-m isobath and the shelf break. The vector-mean current in this regime is directed to the northwest with magnitudes of 1-10 cm/s, and there is a statistically significant ($\sim$1-5 cm/s) cross-shelf component.

The main source of the tidal wave in the Bering Sea is the northern Pacific Ocean; the Arctic Ocean is a secondary source. Tidal currents vary with location. On the southern and central shelf, tides are predominantly semidiurnal and account for $\geq$80% of the total fluctuating kinetic energy. The relative importance of the semidiurnal component of tidal flow in relation to the total tidal flow is reduced on the northeastern shelf, as is the percentage of the total flow accounted for by tides. Tides near Norton Sound are almost purely diurnal, although semidiurnal tidal components reappear to the northwest (Pearson et al., 1981), and are dominant in Anadyr Strait (Coachman et al., 1975).

## 3. METHODS

Data were collected using RCM-4 Aanderaa current meters on taut-wire moorings. Except for two moorings--BC-22 and BC-26, on which meters were at 50 m depth in 76 and 119 m of water, respectively, meters were located nominally 10 m above the bottom. At NC-24 and BC-20 a second meter was located about 20 m below the sea surface. Problems inherent in the use of this type of mooring are discussed in Kinder and Schumacher (1981).

Analyses encompassed the period from October to March for which data are available from almost all the meters. The 1980-1981 moorings were not deployed until mid-November, and three of the 1977-1978 meters stopped before the end of March. The record from BC-21A (1977) was so short that it was not used for comparisons. Other short records were analyzed over the portion of record that was in a common time-span. All current data were filtered, using either a 2.86-hr or a 35-hr symmetrical Lanczos filter, depending on the frequency of interest. The characteristics of the filters and routines in the Rapid Retrieval Data Display or "R2D2" system are discussed in Pearson (1981). Vector plots of the 35-hr data are shown in Figures 3a, b, and c. R2D2 routines were also used to determine the magnitudes and phases of the K1, M2, O1, P1, N2, and S2 tidal constituents over the first common 29-day period of each year's records. The tidal currents produced from these components (Fig. 4a, b, and c) illustrate the nature of the tidal currents and their relative magnitudes along the shelf. Mean scalar current speed, vector-mean speed and direction, and variance on the principal axis (axis of greatest variance) were computed from 35-hr data, and are tabulated in Table 2. Shown in Figures 5 and 6 are the current roses and summary vectors for the 35-hr data, displaying the spatial variations in the directional variability of the currents.

Correlation coefficients and coherence estimates were calculated using the velocity component along the axis of greatest variance of the 35-hr data. Correlation coefficients are listed in Table 3 and composite graphs of the coherence of the central mooring of each year's array with the other moorings are shown in Figures 7a, b, and c, with vertical coherence at two moorings shown in Figure 8.

Following the procedure outlined by Kinder and Schumacher (1981), the partitioning of kinetic energy per unit mass among three frequency bands was examined. The kinetic energy was estimated by $KE(f) = \frac{1}{2}(cw^2+ccw^2)^{\frac{1}{2}}$, where f is a selected frequency band, and cw and ccw are the variance of the clockwise and counterclockwise rotating components. Rotary spectra of 2.86-hr data were computed to calculate the total fluctuating kinetic energy ($KE_{tot}$), and the tidal kinetic energy ($KE_{tid}$). The ratio of the kinetic energy at diurnal and semi-diurnal frequencies was also computed. Rotary spectra of 35-hr data, with a high-frequency cut-off of two days, were used to calculate the amount of kinetic energy at frequencies longer than two days ($KE_L$). Energy in the portion of this band from 2-10 days, usually ascribed to meteorological forcing, was also tabulated ($KE_M$). The result of these computations is presented in Table 4, and some representative spectra are plotted in Figure 9.

To delineate the contribution of atmospheric forcing to the currents, wind fields were calculated from surface atmospheric pressure analyses of 0 and 12 GMT during 1977-1978 using routines in METLIB (Overland et al., 1980). Surface pressure was digitized on a grid which is compatible with the National Meteorological Center's Primi-

tive Equation Grid and then the values were interpolated to quarter mesh to form the basis for gradient wind calculations for each field. The gradient wind was then rotated 30° to the left, and its magnitude decreased by 20% to calculate the surface wind. Vector plots of METLIB winds are shown in Figure 10. Spectra of METLIB winds at the four moorings in the water in 1977-1978 are displayed in Figure 11 while the wind mean speed, vector-mean speed and direction, and variance along the axis of greatest variance are included in Table 2.

An assessment of the effect of ice cover on currents was made using the NOAA/Navy weekly sea-ice extent charts to determine when meters were ice-covered. Since sites NC-24A and BC-20A 1977-1978 were ice-free in October-November and under ice in January-February (Table 1), a comparison of the statistical parameters and the correlation of the currents and wind during those two periods was used to examine the effect of ice-cover on wind-driven circulation (Table 5).

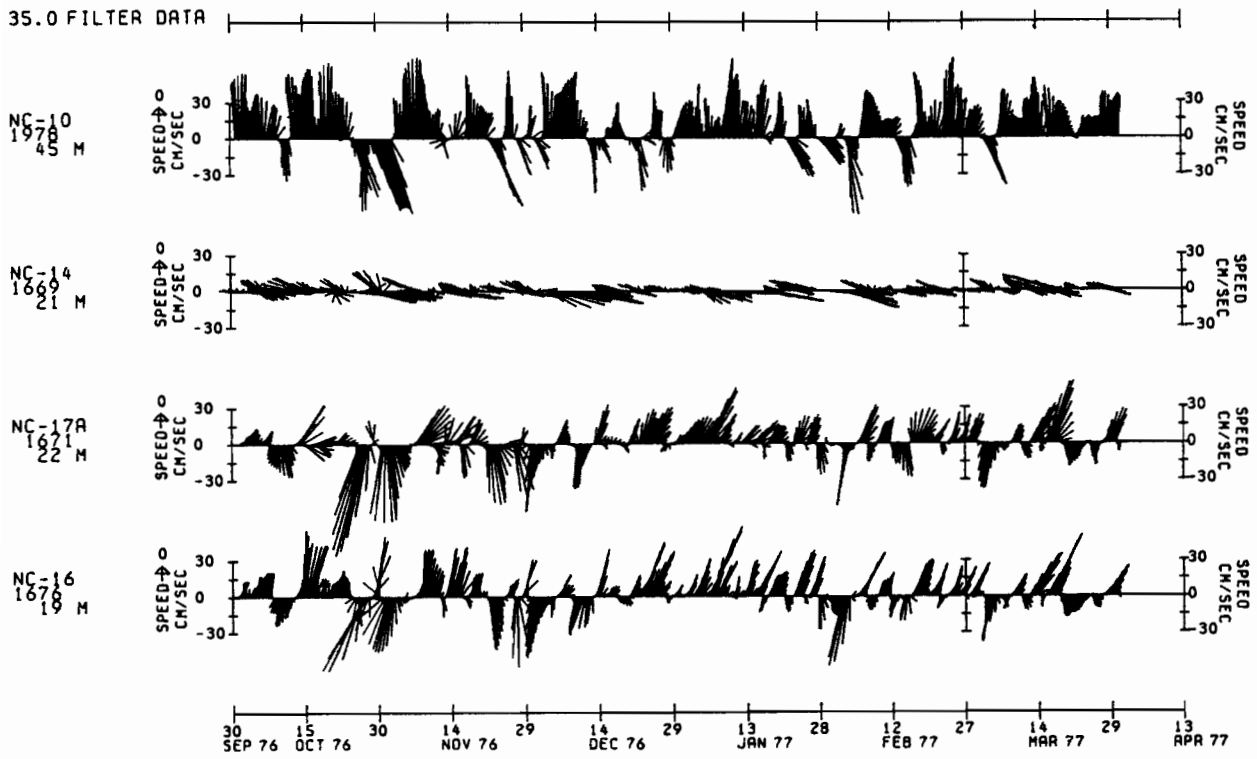


Figure 3a. Stick vector representations of the 35-hour-filtered currents at each meter for 1976-1977. The data spacing is one point every 6 hours.

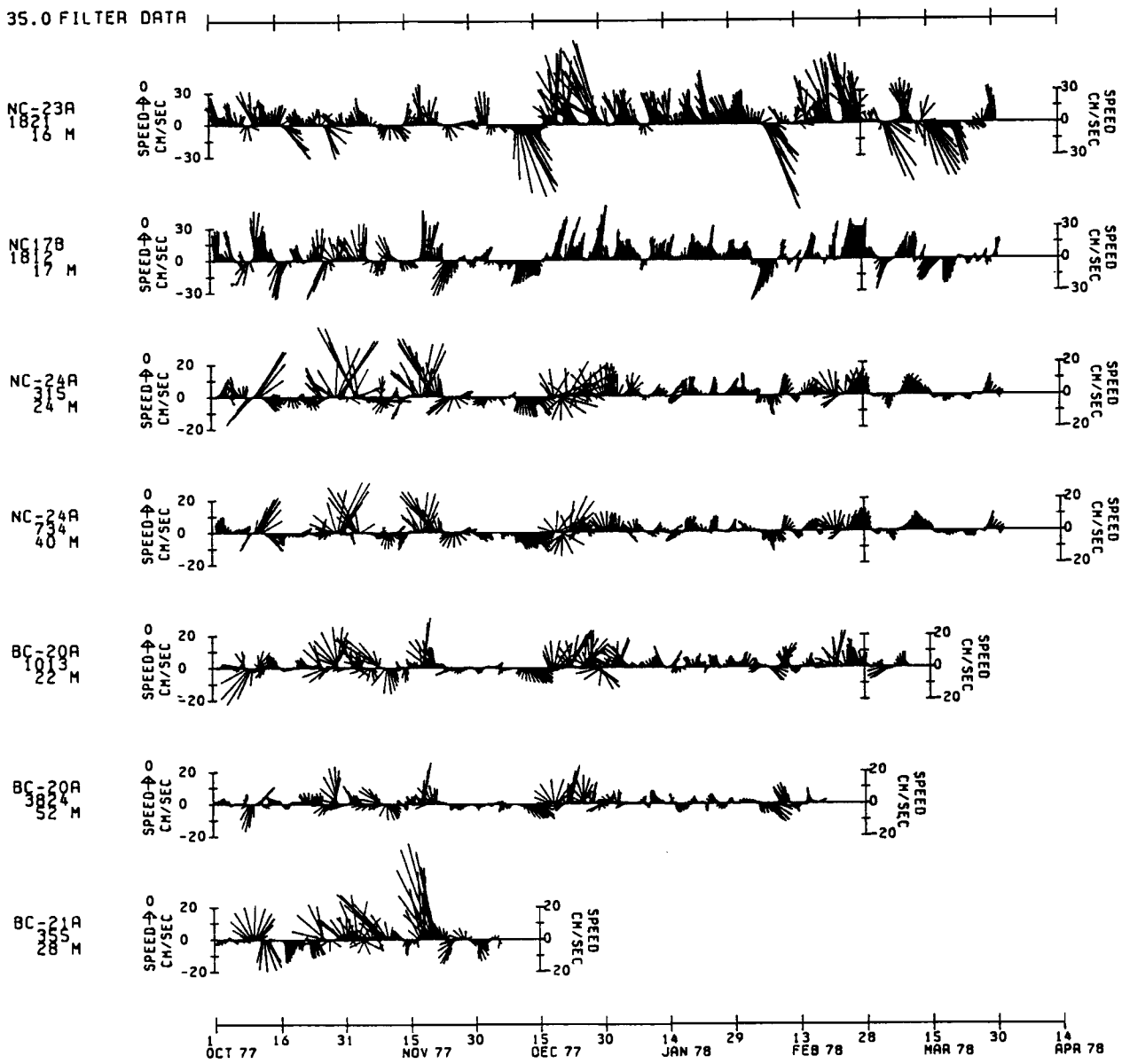


Figure 3b. Stick vector representations of the 35-hour-filtered currents at each meter for 1977-1978. The data spacing is one point every 6 hours.

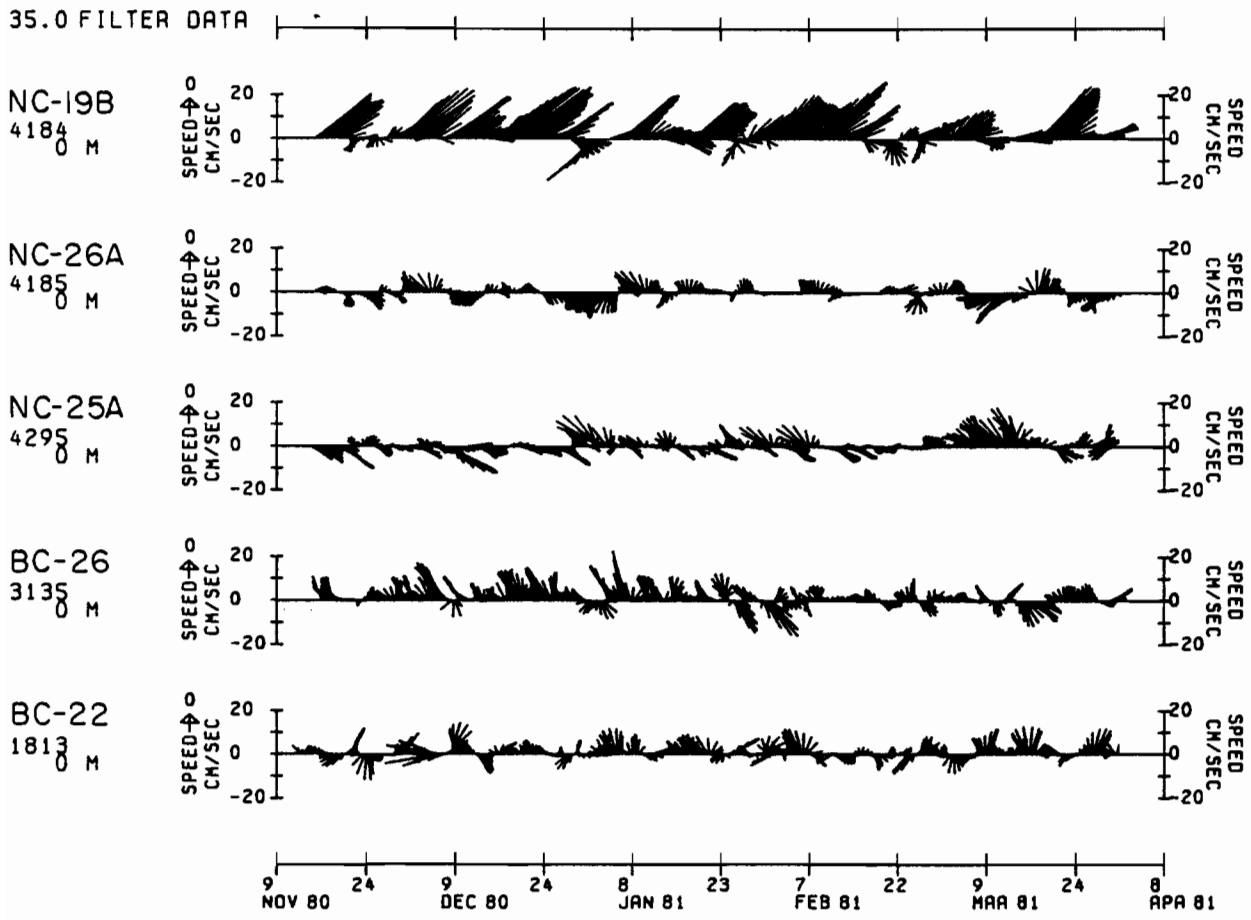


Figure 3c. Stick vector representations of the 35-hour-filtered currents at each meter for 1980-1981. The data spacing is one point every 6 hours.

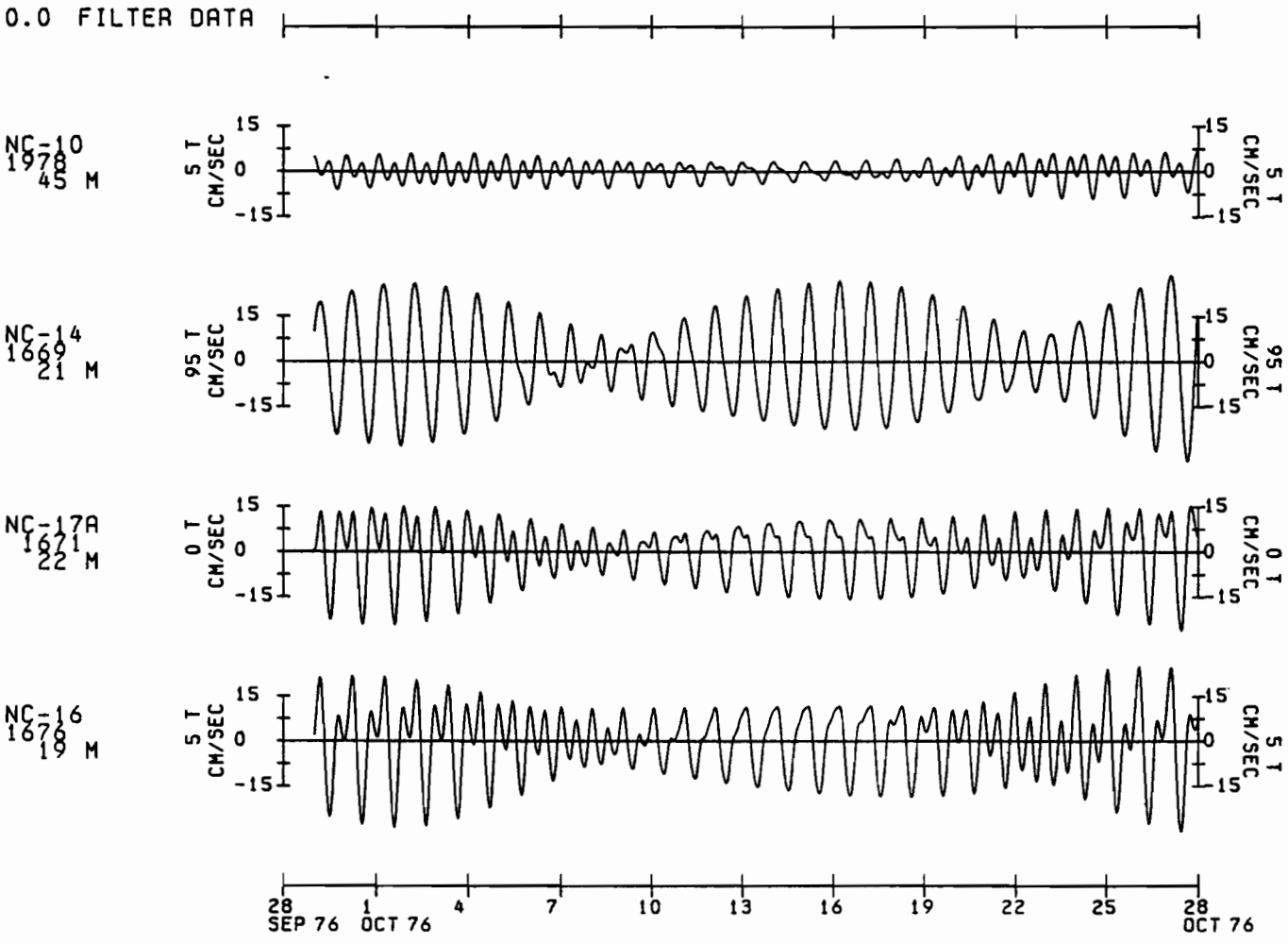


**Figure 4a. The along-isobath component of the tidal current for 1976-1977.**

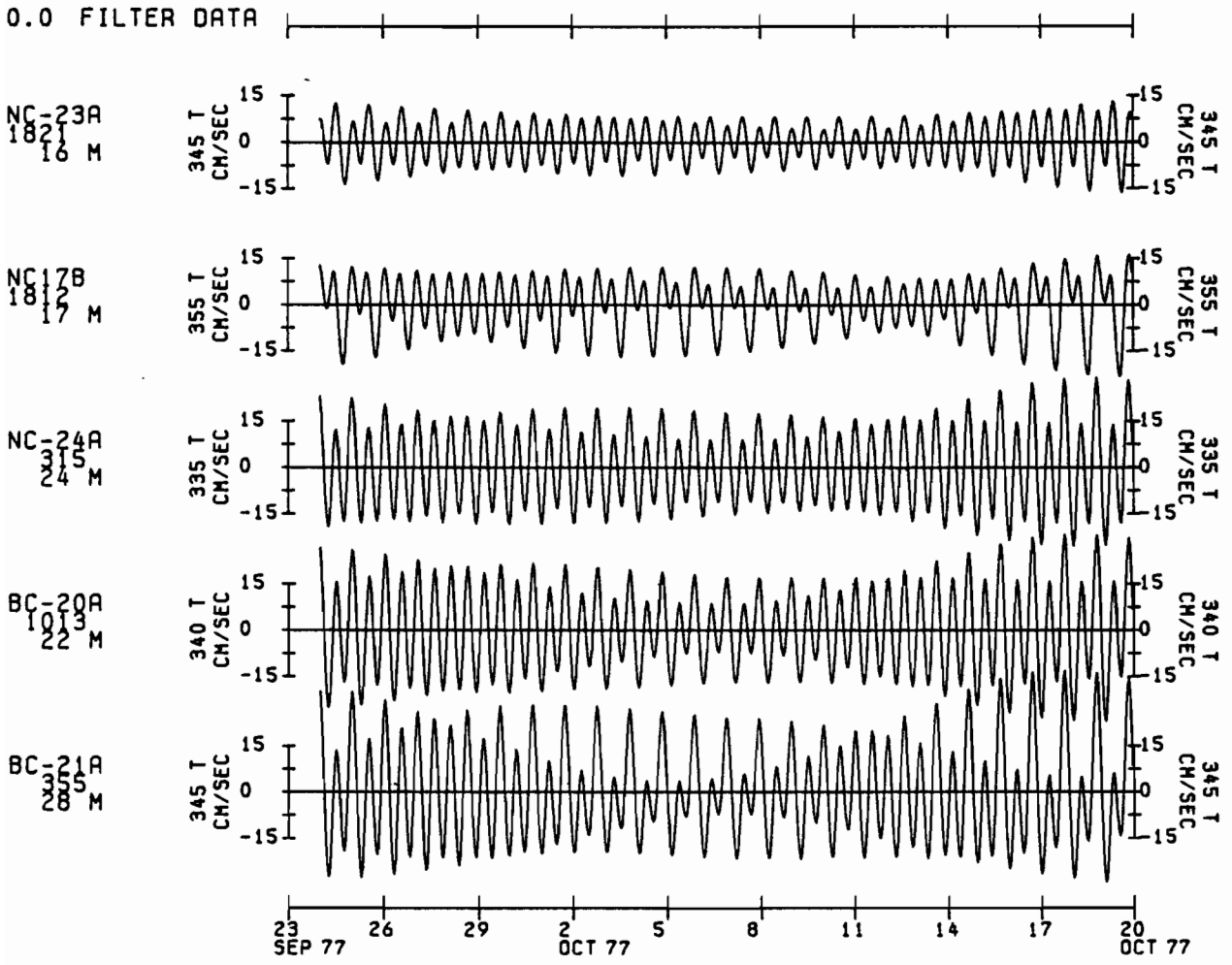


Figure 4b. The along-isobath component of the tidal current for 1977-1978.

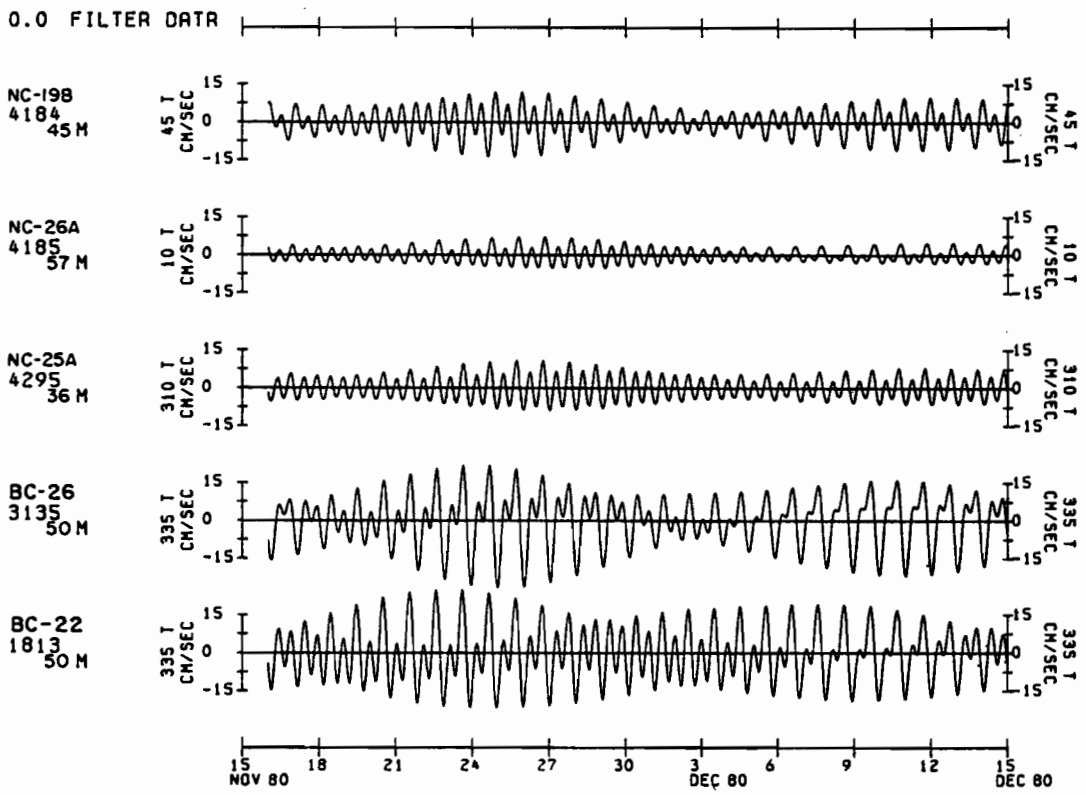


Figure 4c. The along-isobath component of the tidal current for 1980-1981.

Table 2. Statistics of mean currents and surface winds.

| Station | Scalar Mean Speed (cm/s) | Scalar Mean Var. ($cm^2/s^2$) | Vector Mean Speed±E[1] (cm/s) | Vector Mean Direction (°T) | Principal Axis (°T) | Var. on Axis ($cm^2/s^2$) | % of Total Var. |
|---|---|---|---|---|---|---|---|
| | | | 1976-1977 | | | | |
| NC-10 | 28.6 | 232.0 | 15.7±5.6 | 012 | 353 | 783.9 | 97.7 |
| NC-14 | 15.3 | 143.8 | 4.5±4.2 | 085 | 103 | 848.1 | 97.6 |
| NC-17A | 16.2 | 176.9 | 4.4±1.3 | 103 | 013 | 392.4 | 93.4 |
| NC-16 | 18.0 | 172.9 | 5.9±4.5 | 035 | 015 | 444.8 | 96.5 |
| | | | 1977-1978 | | | | |
| NC-23A | 21.5 | 251.4 | 10.2±6.8 | 357 | 338 | 548.8 | 90.3 |
| NC-17B | 15.2 | 106.9 | 7.2±4.4 | 354 | 009 | 267.8 | 93.4 |
| NC-24A | 8.9 | 54.0 | 3.2±2.1 | 012 | 000 | 78.5 | 64.1 |
| NC-24A | 7.1 | 29.7 | 1.9±1.3 | 033 | 356 | 49.1 | 64.5 |
| BC-20A | 7.9 | 34.7 | 3.7±1.7 | 334 | 359 | 50.9 | 60.8 |
| BC-20A | 5.7 | 20.5 | 1.4±1.5 | 350 | 346 | 33.6 | 66.6 |
| *BC-21A | 10.9 | 107.4 | 3.1±4.8 | 326 | 343 | 181.1 | 83.6 |
| | | | WIND | | | | |
| NC-23A | 8.9 | 19.5 | 5.5±0.8 | 232 | 170 | 43.8 | 65.1 |
| NC-17B | 9.1 | 18.8 | 5.2±0.8 | 233 | 160 | 44.3 | 60.3 |
| NC-24A | 9.5 | 19.3 | 5.2±0.9 | 227 | 143 | 49.3 | 60.5 |
| BC-20A | 9.4 | 18.6 | 4.5±0.5 | 229 | 137 | 52.1 | 60.3 |
| | | | 1980-1981 | | | | |
| NC-19B | 16.8 | 78.8 | 14.0±3.8 | 061 | 044 | 149.7 | 92.1 |
| NC-26A | 5.1 | 12.3 | 0.8±1.9 | 216 | 211 | 23.8 | 63.2 |
| NC-25A | 7.3 | 23.4 | 2.5±1.8 | 085 | 123 | 62.1 | 87.9 |
| BC-26 | 7.0 | 17.6 | 3.8±2.3 | 341 | 328 | 42.6 | 80.7 |
| BC-22 | 5.7 | 12.8 | 2.1±1.0 | 345 | 019 | 22.5 | 55.5 |

*Short record.

[1]R.M.S. Error, $E = \pm 2\,\sigma/(T/\tau)^{\frac{1}{2}}$ where T is the record length, $\sigma$ the standard deviation along the vector mean axis and $\tau$ is an estimate of the area under the autocorrelation function.

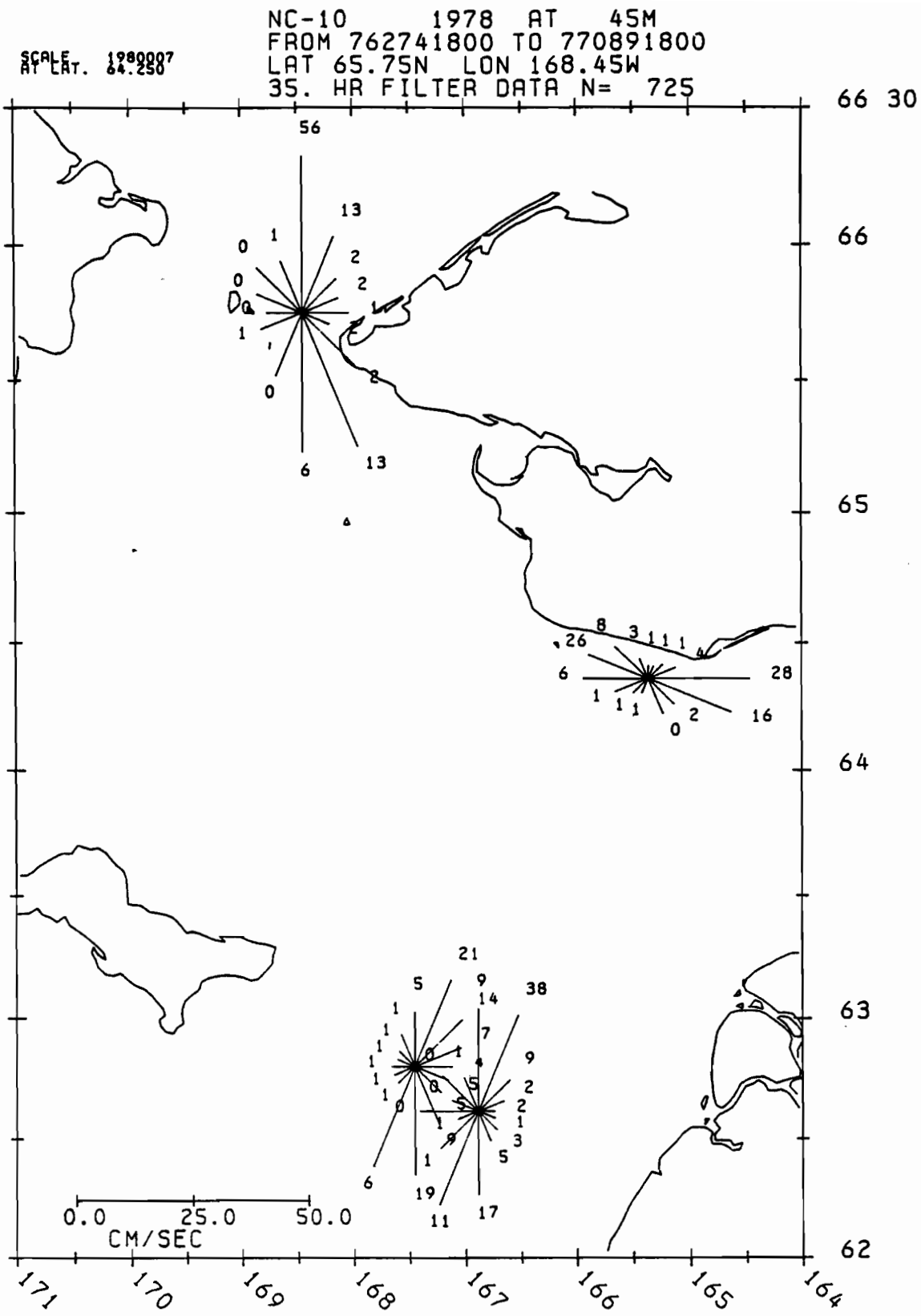


Figure 5a. Current roses for 1976-1977, where direction is divided into 16 bins. The percent of observations within each bin is indicated by the number at the end of each line, and the length of the line indicates the mean speed of currents within that bin.

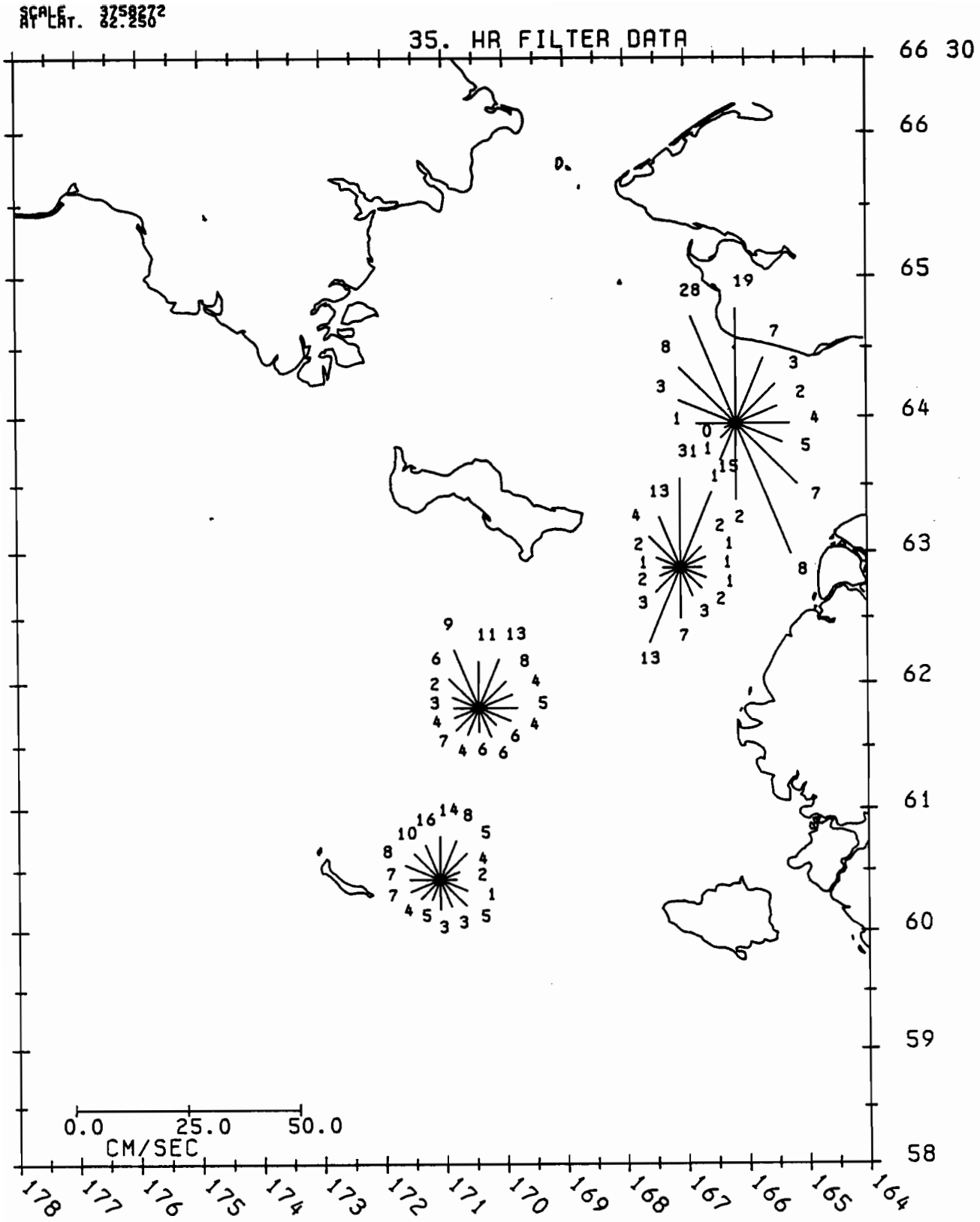


Figure 5b. Current roses for 1977-1978, where direction is divided into 16 bins. The percent of observations within each bin is indicated by the number at the end of each line, and the length of the line indicates the mean speed of currents within that bin.

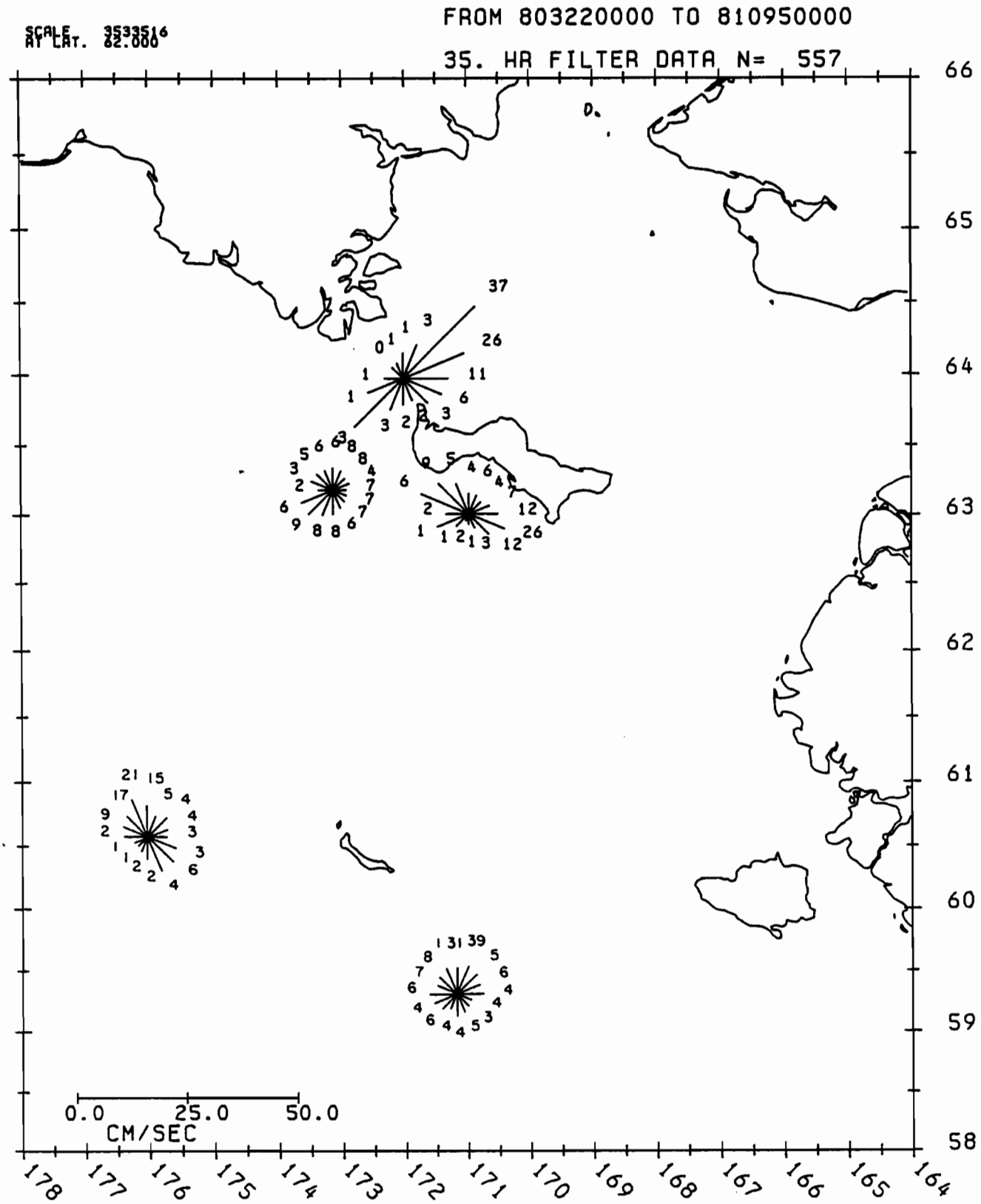


Figure 5c. Current roses for 1980-1981, where direction is divided into 16 bins. The percent of observations within each bin is indicated by the number at the end of each line, and the length of the line indicates the mean speed of currents within that bin.

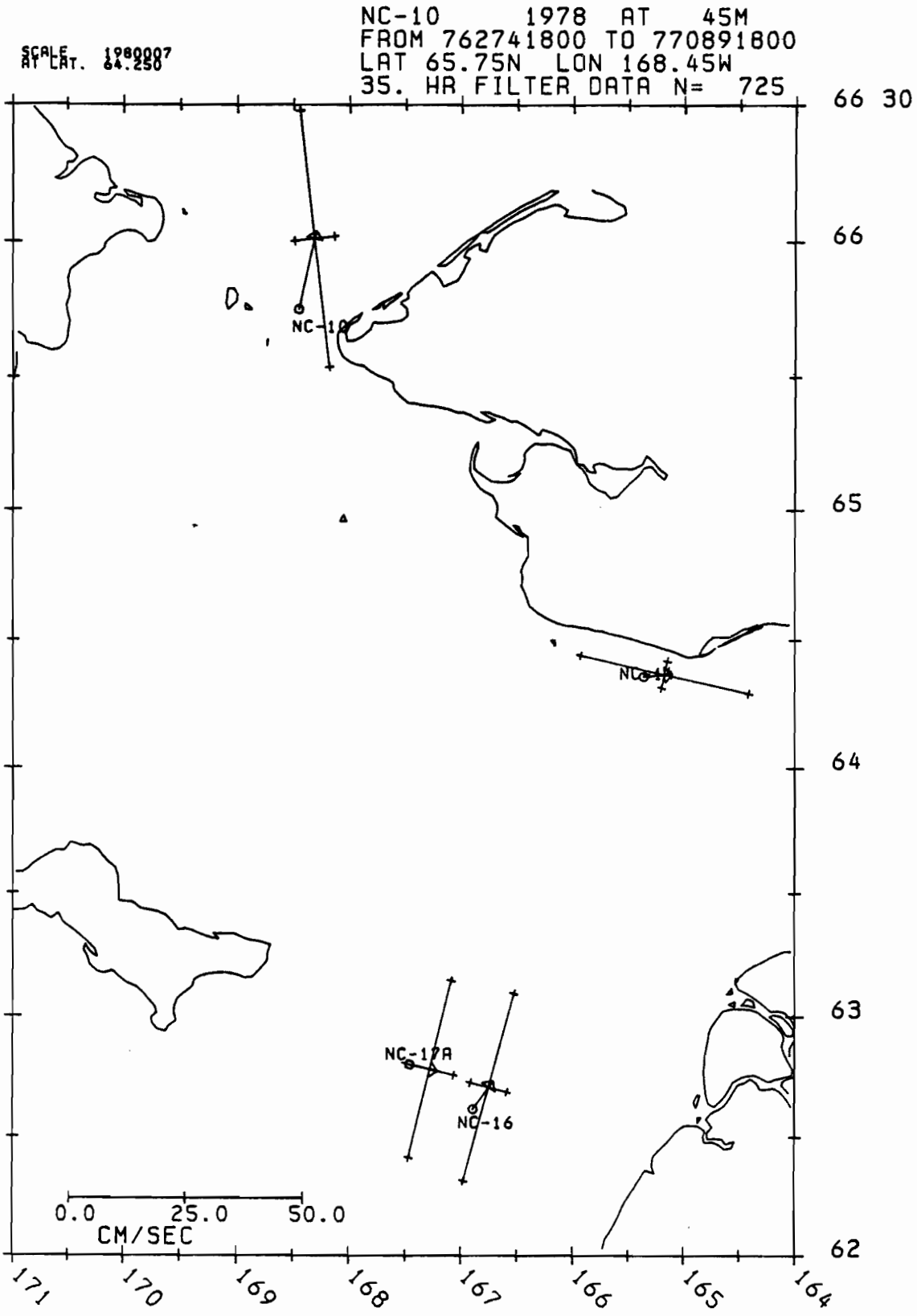


Figure 6a. Vector mean flow for 1976-1977. The circle is at the mooring site. The crossbars located at the barb of the arrow show the principal axis of flow and its complement. The lengths of the crossbars are proportional to the variance occurring along each axis.

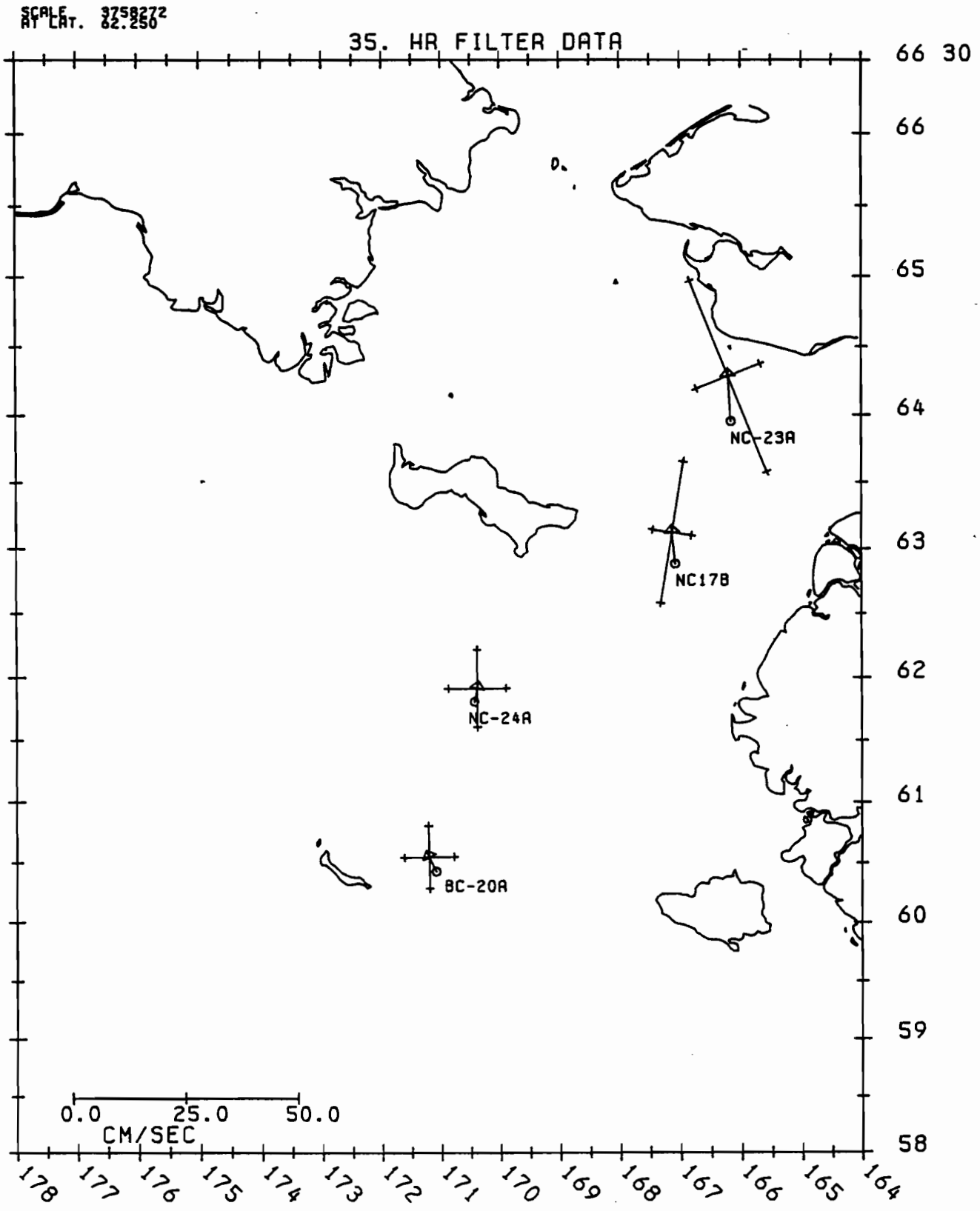


Figure 6b. Vector mean flow for 1977-1978. The circle is at the mooring site. The crossbars located at the barb of the arrow show the principal axis of flow and its complement. The lengths of the crossbars are proportional to the variance occurring along each axis.

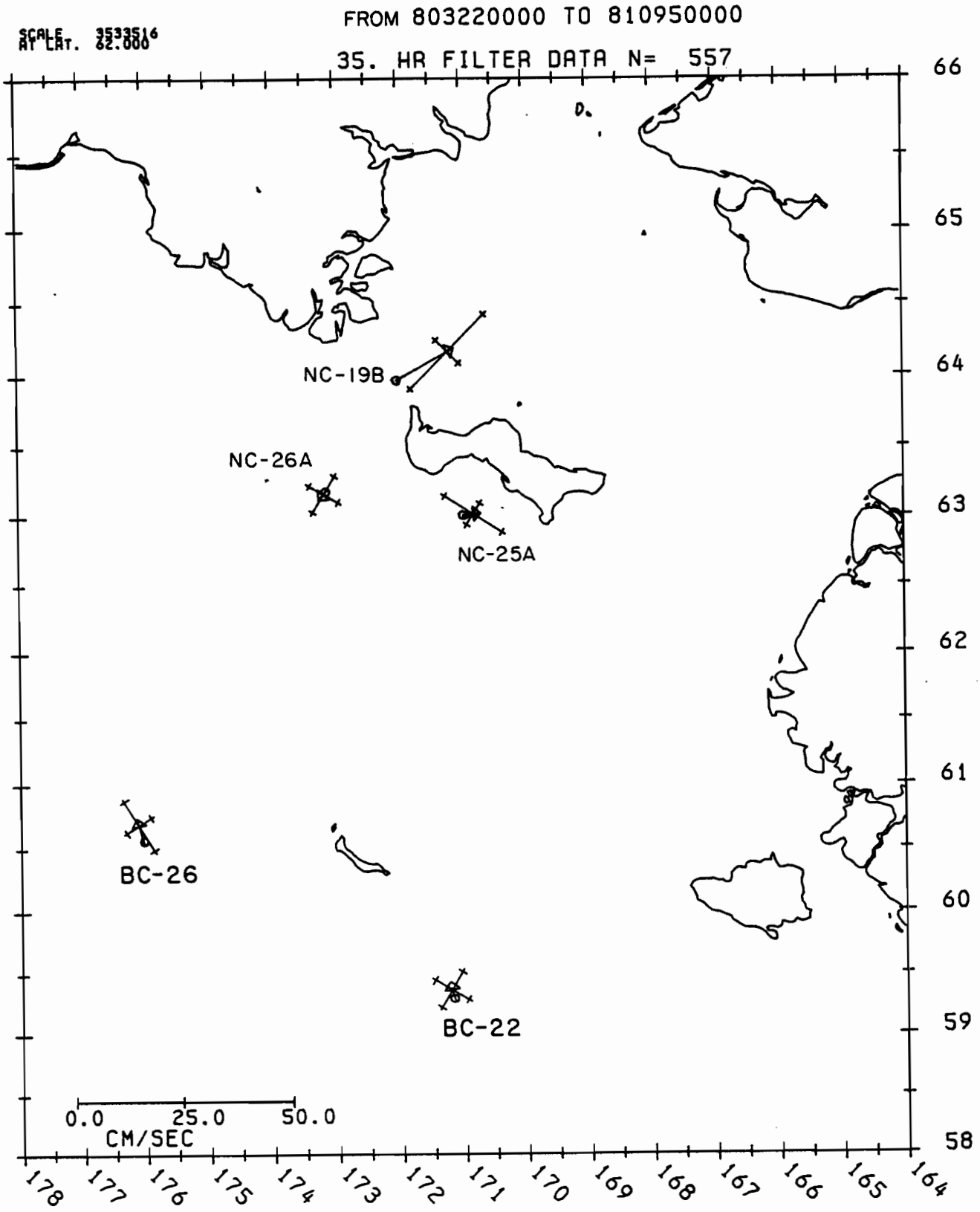


Figure 6c. Vector mean flow for 1980-1981. The circle is at the mooring site. The crossbars located at the barb of the arrow show the principal axis of flow and its complement. The lengths of the crossbars are proportional to the variance occurring along each axis.

Table 3. Correlation coefficients between current records. Coefficients with an * improved when the northern record lagged the southern record, and correlations marked with a √ were better when the northern record led the southern one.

| 1976-1977 | NC-10 NC-14 | NC-10 NC-17A | NC-10 NC-16 | NC-14 NC-17A | NC-14 NC-16 | NC-17A NC-16 |
|---|---|---|---|---|---|---|
| Distance(km) | 236 | 332 | 356 | 173 | 207 | 35 |
| Correlation | -0.3 | 0.5* | 0.4* | -0.1* | -0.2 | 0.9 |
| 95% level | 0.2 | 0.2 | 0.2 | 0.2 | 0.2 | 0.2 |

| 1977-1978 | NC-23A NC-17B | NC-23A NC-24A | NC-23A BC-20A | NC-17B NC-24A | NC-17B BC-20A | NC-24A BC-20A | Vertical NC-24A | Vertical BC-20A |
|---|---|---|---|---|---|---|---|---|
| Distance(km) | 127 | 324 | 468 | 213 | 347 | 157 | 0 | 0 |
| Correlation | 0.8* | 0.5* | 0.4* | 0.6 | 0.5 | 0.7 | 0.9 | 0.9* |
| 95% level | 0.3 | 0.2 | 0.2 | 0.2 | 0.2 | 0.2 | 0.2 | 0.2 |

| Wind, 1977-1978 | NC-23 | NC-17B | NC-24A (upper) | NC-24A (lower) | BC-20A (upper) | BC-20A (lower) |
|---|---|---|---|---|---|---|
| Correlation | 0.6 | 0.7 | 0.4 | 0.3 | 0.3 | 0.4 |
| 95% level | 0.3 | 0.2 | 0.2 | 0.2 | 0.2 | 0.2 |

| 1980-1981 | NC-19B NC-26A | NC-19B NC-25A | NC-19B BC-26 | NC-19B BC-22 | NC-26A NC-25A | NC-26A BC-26 | NC-26A BC-22 | NC-25A BC-26 | NC-25A BC-22 | BC-22 BC-26 |
|---|---|---|---|---|---|---|---|---|---|---|
| Distance (km) | 104 | 166 | 436 | 520 | 111 | 327 | 442 | 379 | 412 | 304 |
| Correlation | -0.5* | 0.6√ | 0.4 | 0.2√ | -0.5√ | -0.2√ | 0.2 | 0.5* | -0.2* | -0.1* |
| 95% level | 0.3 | 0.3 | 0.2 | 0.2 | 0.3 | 0.2 | 0.2 | 0.2 | 0.2 | 0.2 |

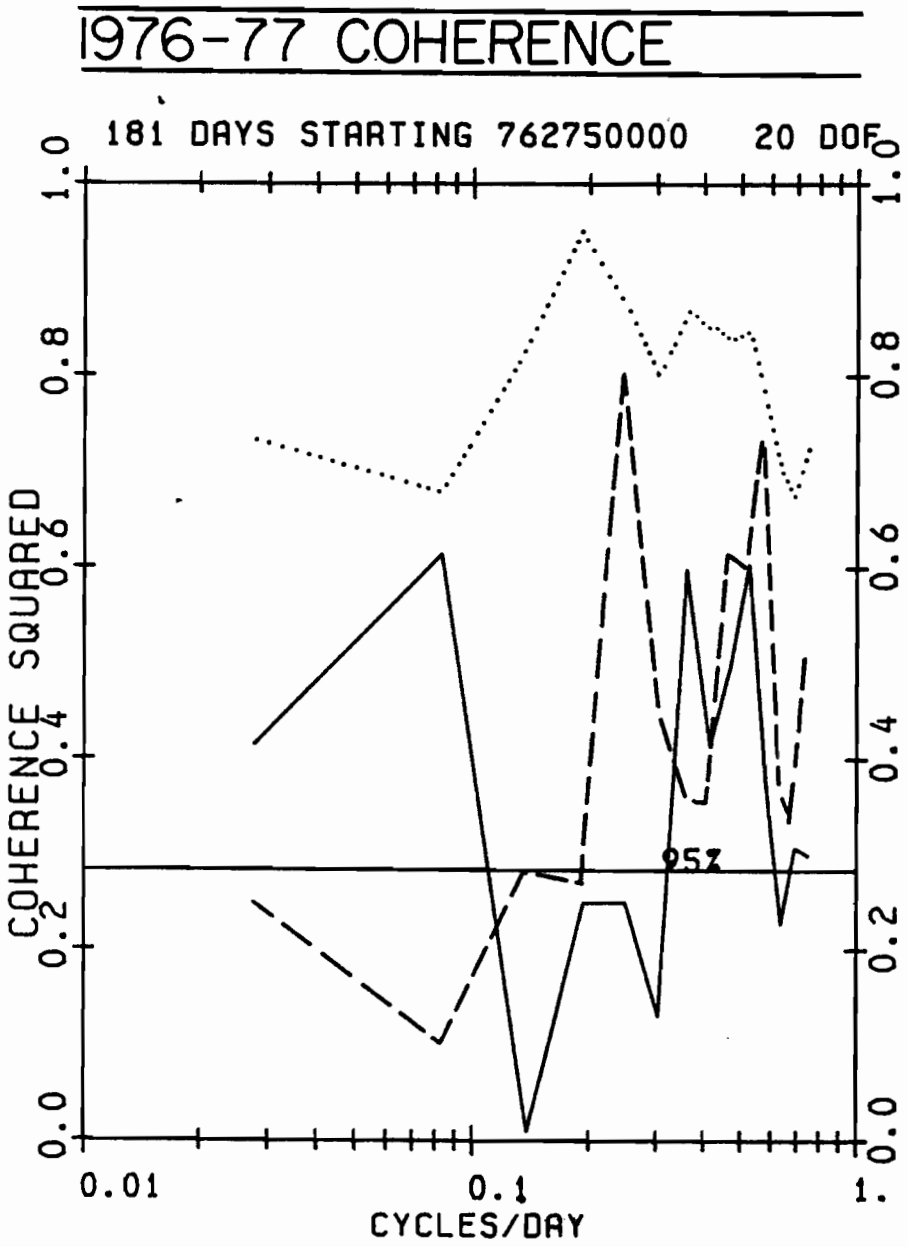


Figure 7a. Composite graphs of the coherence of flow at the central mooring with flow at each of the other sites for 1976-1977. The 95% level is labeled on each graph.

——— Comparison of NC-10 with NC-17A
– – – – Comparison of NC-14 with NC-17A
····· Comparison of NC-17A with NC-16

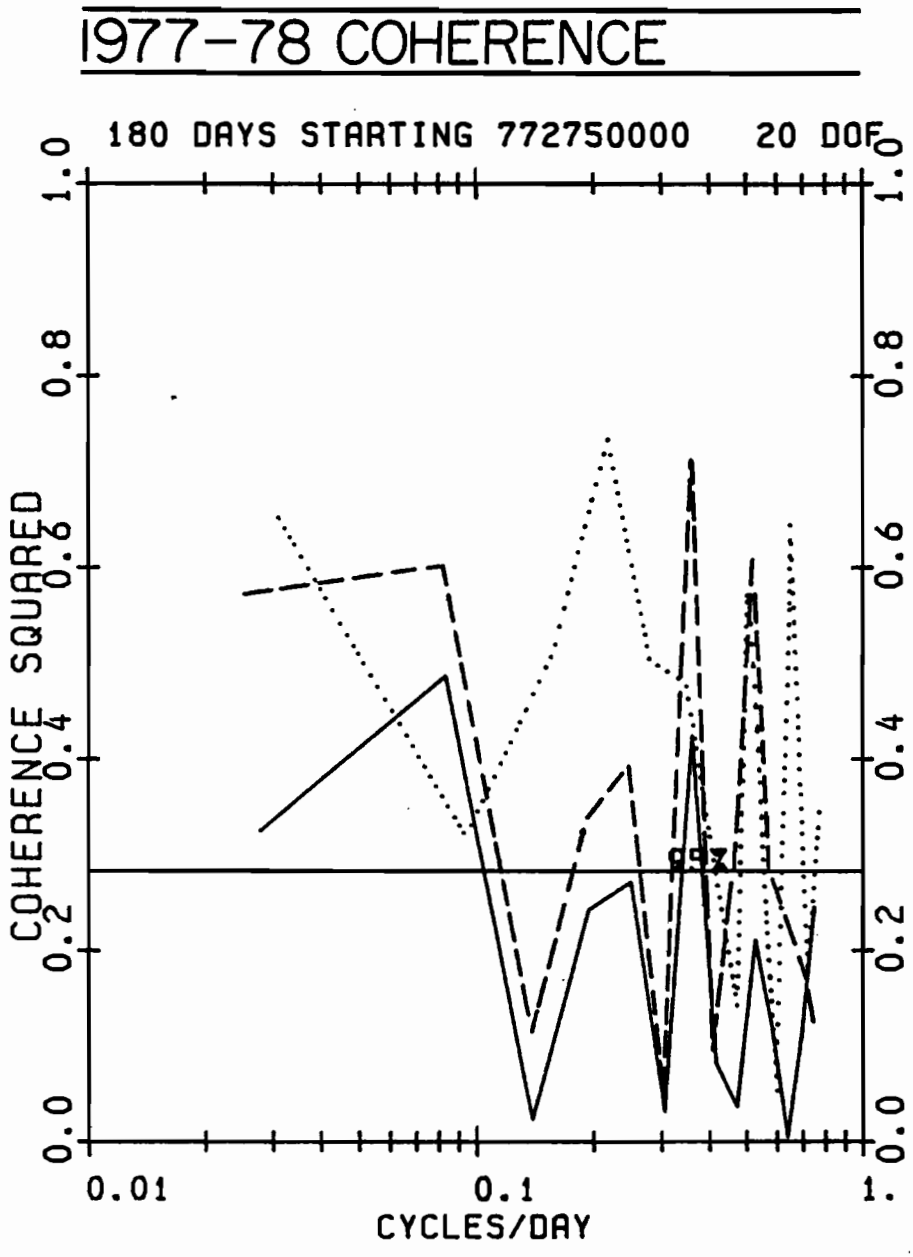


Figure 7b. As in 7a, only for 1977-1978.

——— Comparison of NC-23 with NC-24A
– – – – Comparison of NC-17B with NC-24A
····· Comparison of NC-24A with BC-20A

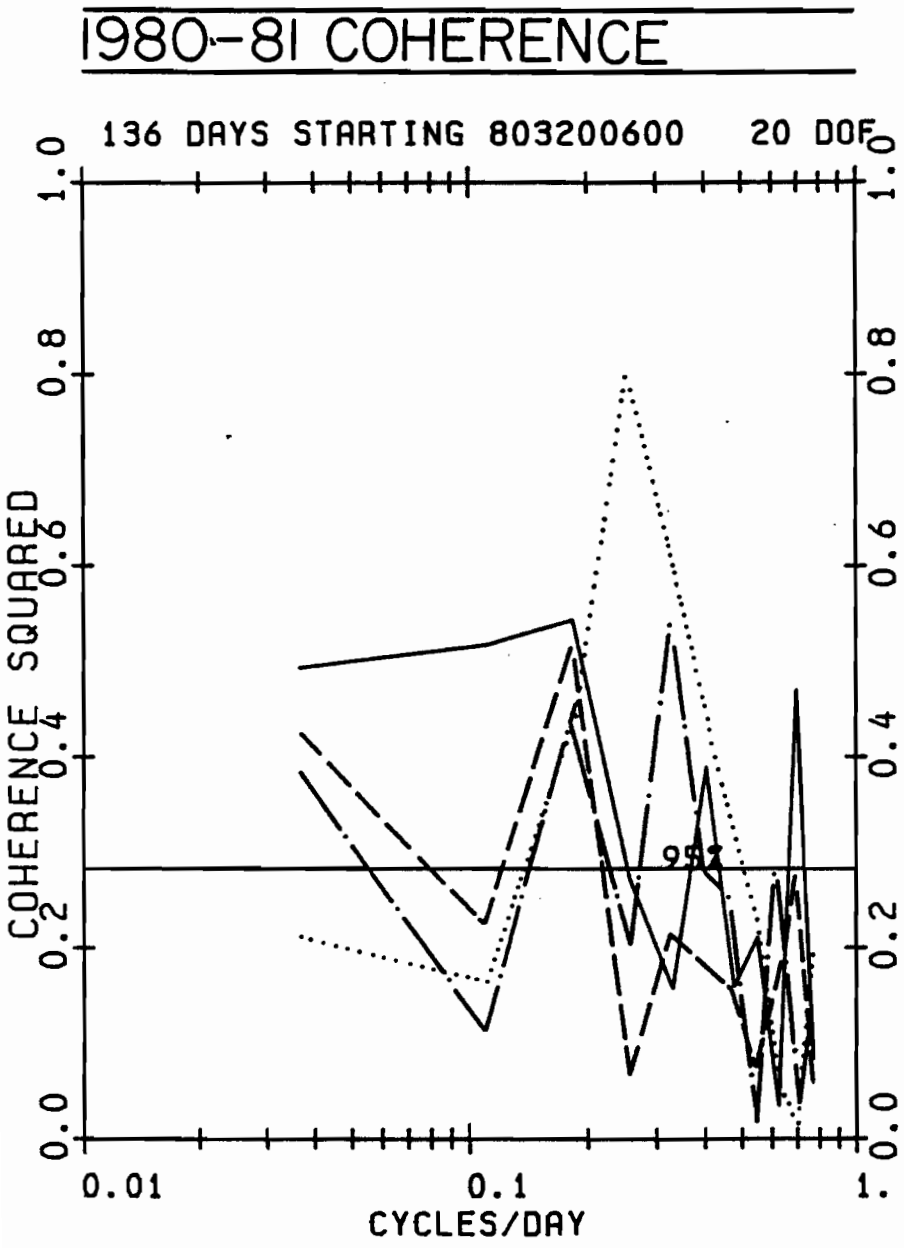


Figure 7c. As in 7a, only for 1980-1981.

——— Comparison of NC-19B with NC-25A
- - - - Comparison of NC-26A with NC-25A
····· Comparison of NC-25A with BC-26
- · - · Comparison of NC-25A with BC-22

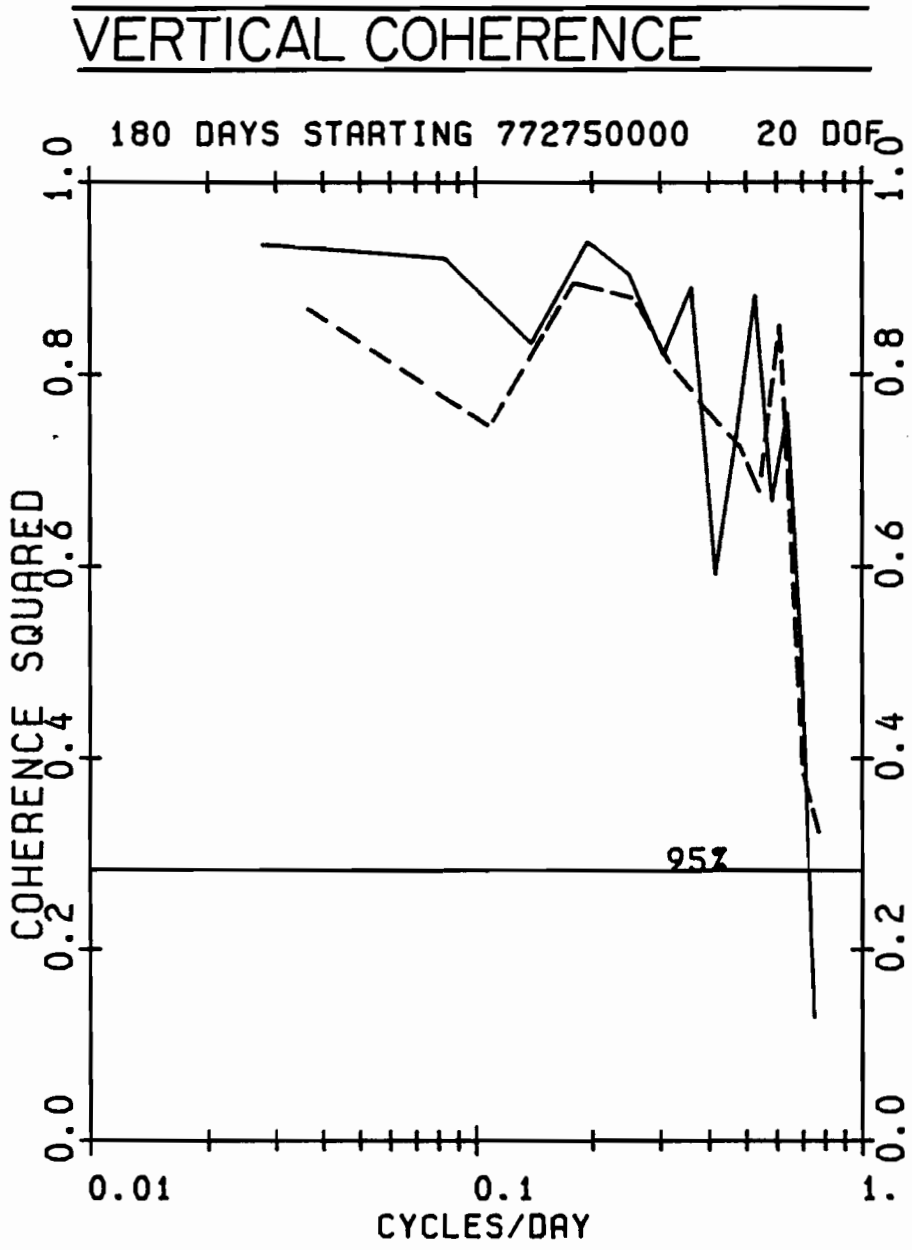


Figure 8. Vertical coherence at the two moorings deployed in 1977-1978 which had two meters.

——— NC-24A
- - - - BC-20A

Table 4. Partition of kinetic energy where $KE_m$ is the kinetic energy at 0.1 to 0.5 cpd, and $KE_L$ is the kinetic energy for frequencies lower than 0.5 cpd, KE' is the total energy of the fluctuations, and $\overline{KE}$ is the kinetic energy of the vector mean flow. Summary by averaging current records north and south of St. Lawrence is also given.

| Station | Total KE' ($cm^2/s^2$) | $\overline{KE}$ | Tidal KE ($cm^2/s^2$) | Tidal (%) | Diurnal / Semidiurnal | $KE_L$ ($cm^2/s^2$) | $KE_M$ ($cm^2/s^2$) | $KE_M/KE_L$ (%) | $KE_L/KE_{Tot}$ (%) |
|---|---|---|---|---|---|---|---|---|---|
| 1976-1977 | | | | | | | | | |
| NC-10 | 454 | 123 | 8 | 1.8 | 1.4 | 423 | 264 | 62.4 | 93.2 |
| NC-14 | 299 | 10 | 97 | 32.4 | 50.5 | 180 | 125 | 69.5 | 60.2 |
| NC-17A | 302 | 10 | 63 | 20.9 | 1.4 | 215 | 149 | 69.3 | 71.2 |
| NC-16 | 386 | 17 | 119 | 30.8 | 1.2 | 237 | 171 | 72.2 | 61.4 |
| 1977-1978 | | | | | | | | | |
| NC-23A | 546 | 52 | 196 | 35.9 | 3.5 | 317 | 178 | 56.2 | 58.1 |
| NC-17B | 241 | 26 | 84 | 34.9 | 1.2 | 143 | 95 | 66.4 | 59.3 |
| NC-24A | 216 | 5 | 127 | 58.8 | 0.1 | 62 | 45 | 72.6 | 28.7 |
| NC-24A | 121 | 2 | 77 | 63.6 | 0.2 | 39 | 28 | 71.8 | 32.2 |
| BC-20A | 281 | 7 | 226 | 80.4 | 0.2 | 41 | 30 | 73.2 | 14.6 |
| BC-20A | 156 | 1 | 123 | 78.8 | 0.3 | 26 | 17 | 65.4 | 16.7 |
| Wind | | | | | ($m^2/s^2$) | ($m^2/s^2$) | | | |
| NC-23A | | | | | 32 | 19 | 59.4 | | |
| NC-17B | | | | | 35 | 20 | 57.1 | | |
| NC-24A | | | | | 39 | 23 | 59.0 | | |
| BC-20A | | | | | 41 | 26 | 63.4 | | |
| 1980-1981 | | | | | | | | | |
| NC-19B | 100 | 98 | 13 | 13 | 0.3 | 83 | 39 | 47.0 | 83.0 |
| NC-26A | 25 | <1 | 4 | 16 | 0.4 | 19 | 9 | 47.4 | 76.0 |
| NC-25A | 47 | 3 | 8 | 17 | 0.2 | 35 | 20 | 57.1 | 74.5 |
| BC-26 | 123 | 7 | 89 | 72.4 | 0.3 | 28 | 16 | 57.1 | 22.8 |
| BC-22 | 183 | 2 | 154 | 84.2 | 0.8 | 20 | 15 | 75.0 | 10.9 |

Summary by Region

| | Total KE | $KE_{Tid}$ | $KE_L$ | $KE_M$ | $KE_M/KE_L$ | $KE_{Tid}/KE_{Tot}$ | $KE_L/KE_{Tot}$ |
|---|---|---|---|---|---|---|---|
| North (n=7) | 332±146 | 83±65 | 228±113 | 146±71 | 63±9 | 24±13 | 69±14 |
| South (n=6) | 109±61 | 76±60 | 28±8 | 18±6 | 62±10 | 55±31 | 39±29 |

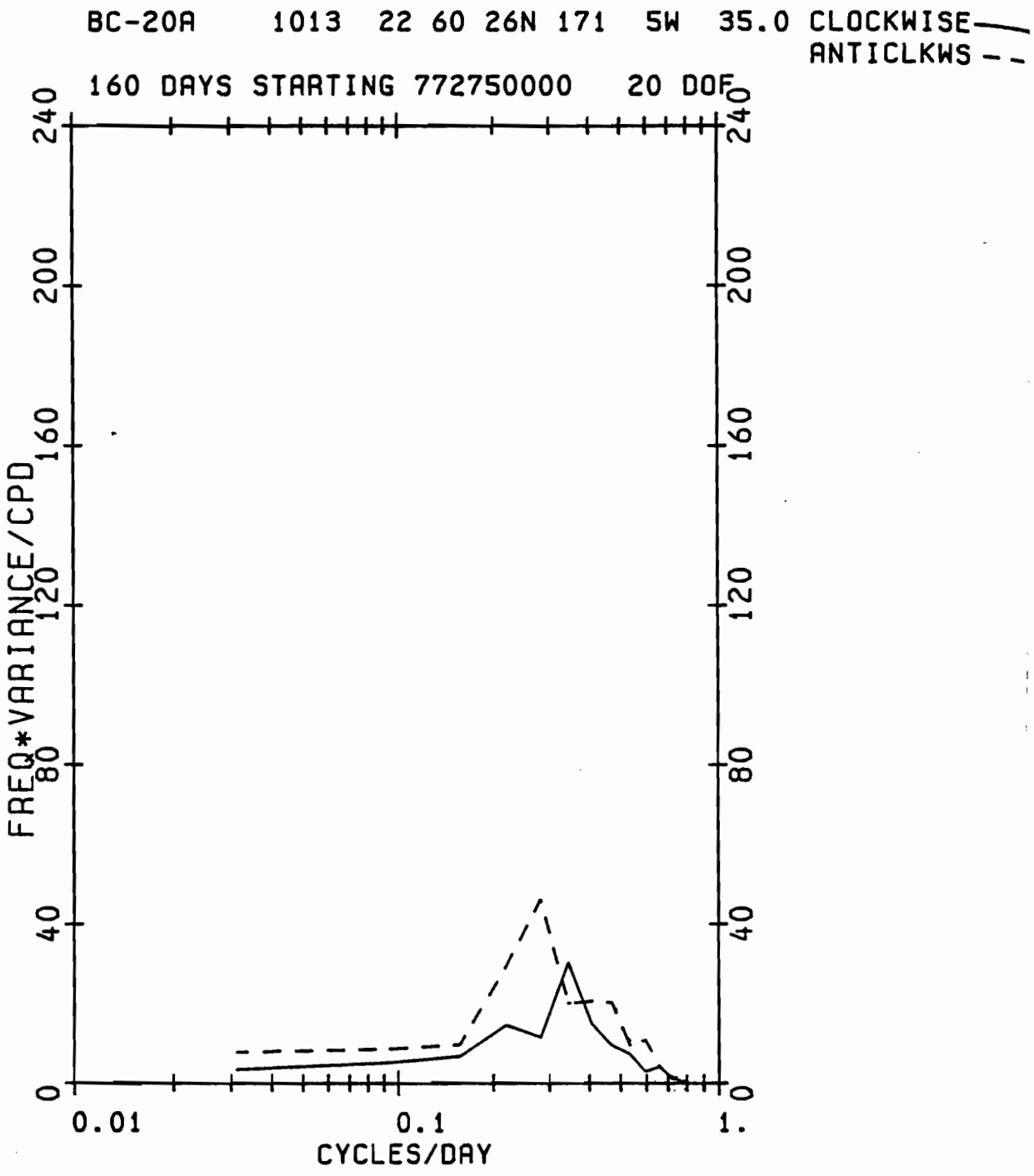


Figure 9a. Representative rotary spectra of 35-hour-filtered data in 1977-1978. Spectra were chosen to illustrate their change as a function of position.

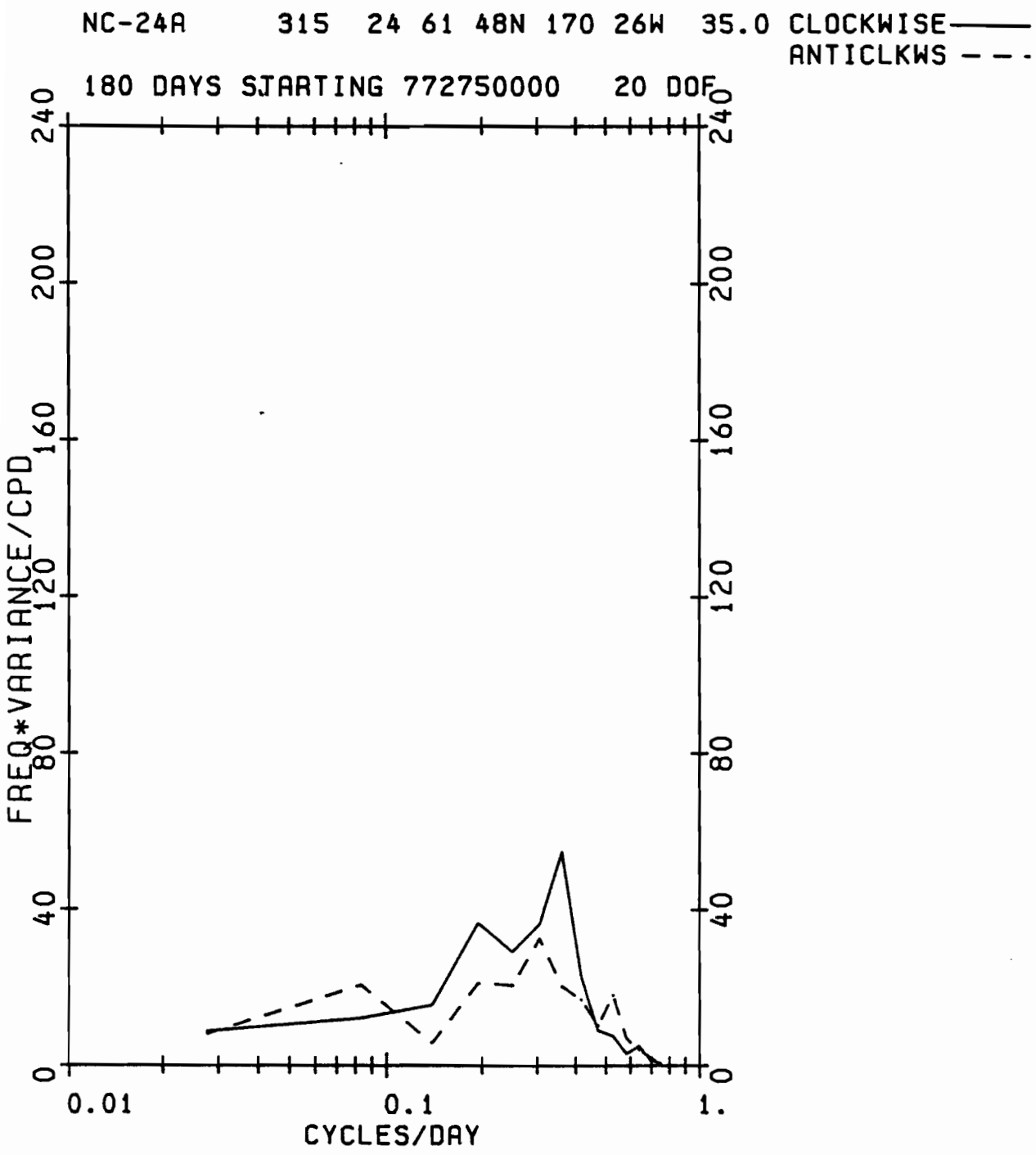


Figure 9b. As in 9a.

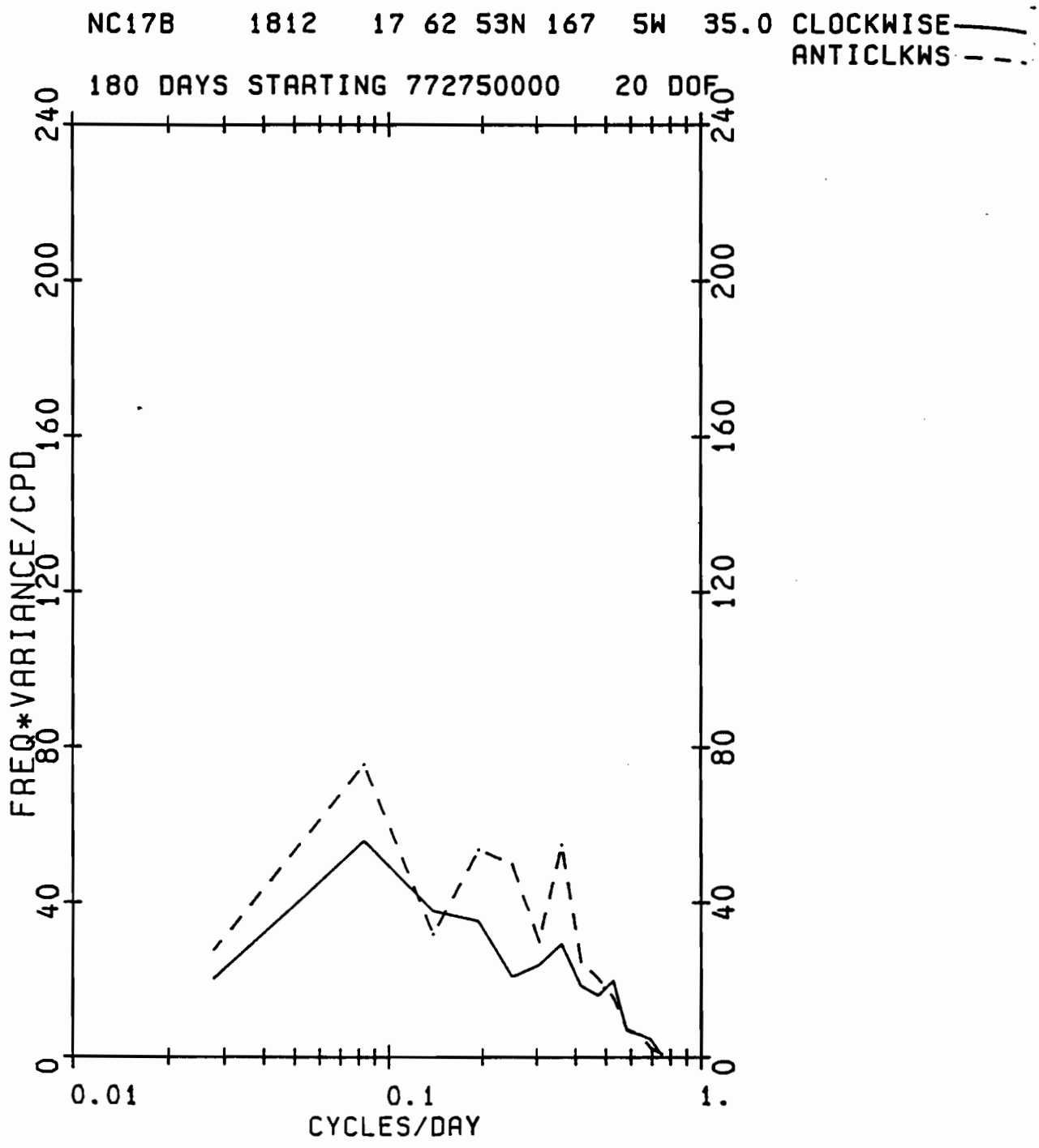


Figure 9c. As in 9a.

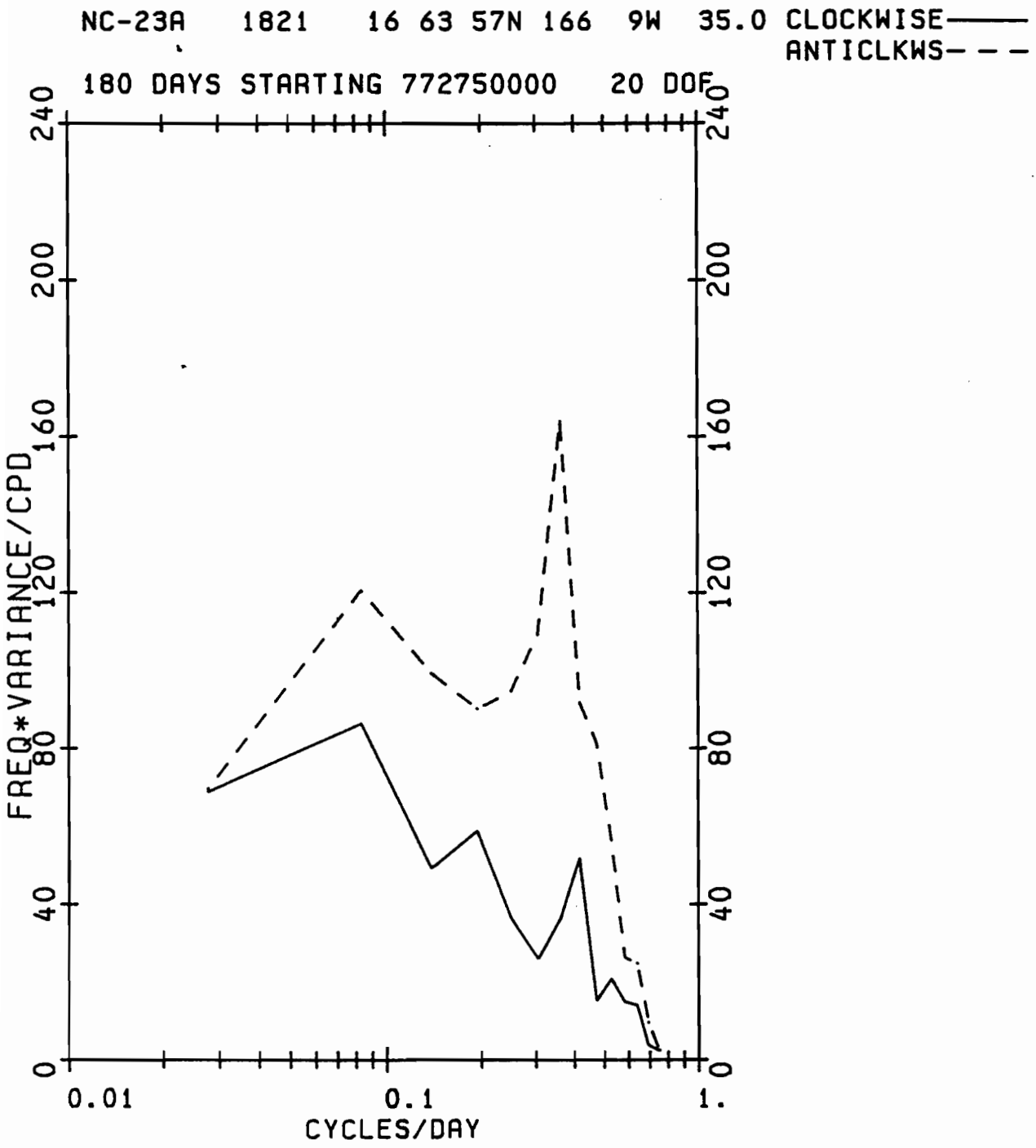


Figure 9d. As in 9a.

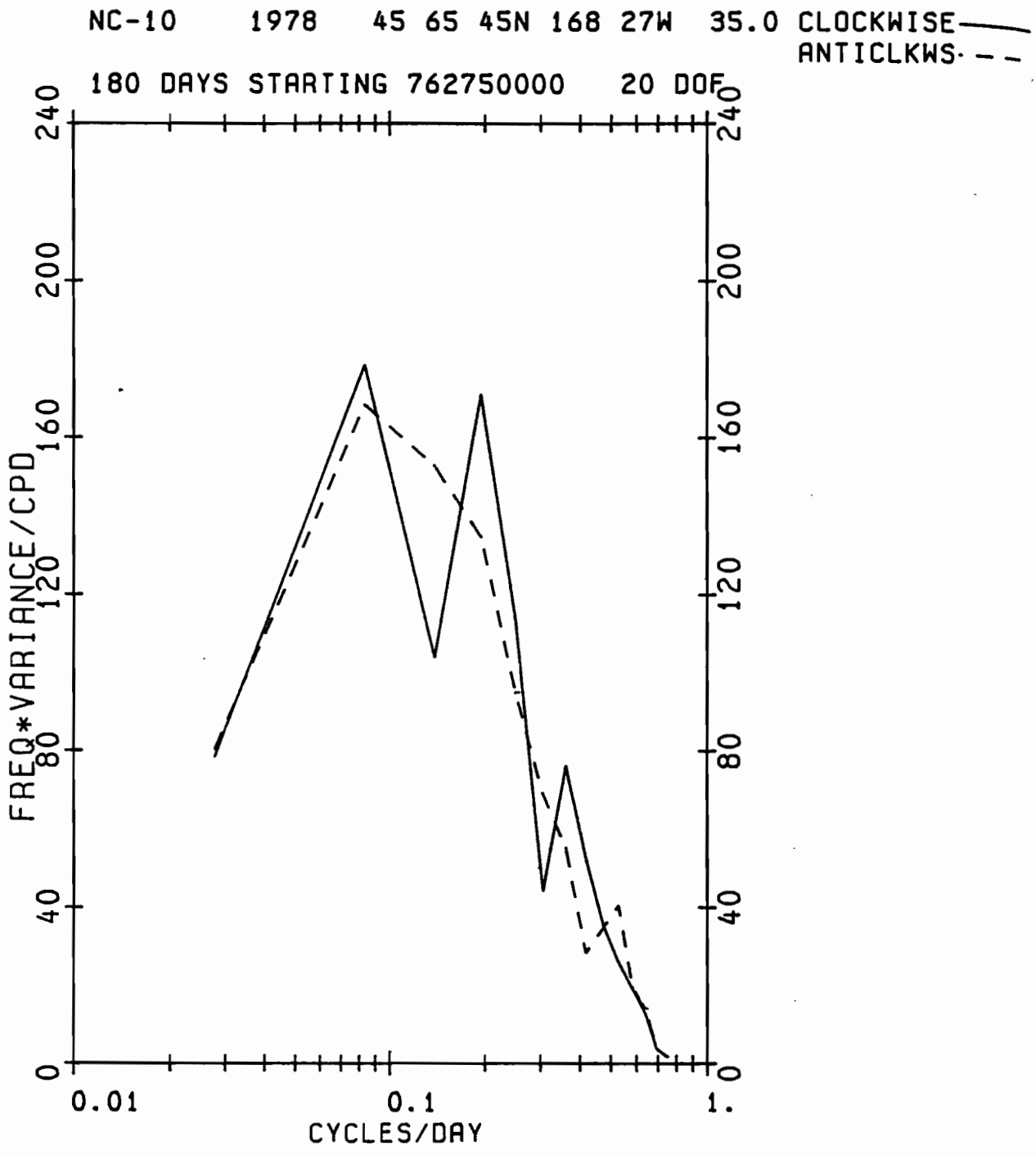


Figure 9e. 1976-1977 spectra illustrate characteristics of meters in a region not included in the 1977-1978 data (9a-9d).

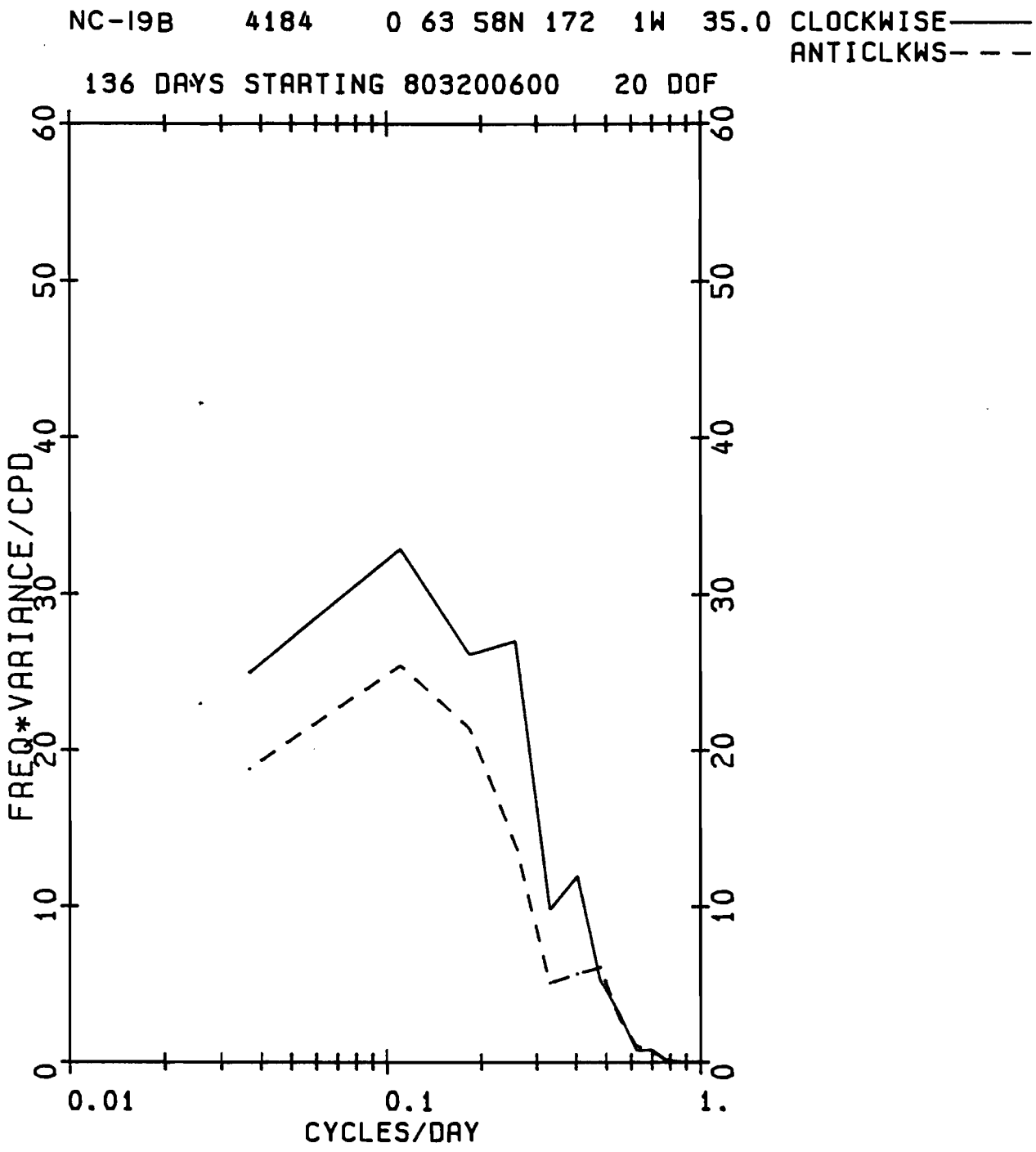


Figure 9f. 1980-1981 spectra illustrate characteristics of meters in a region not included in the 1976-1977 or 1977-1978 data (9a-9e).

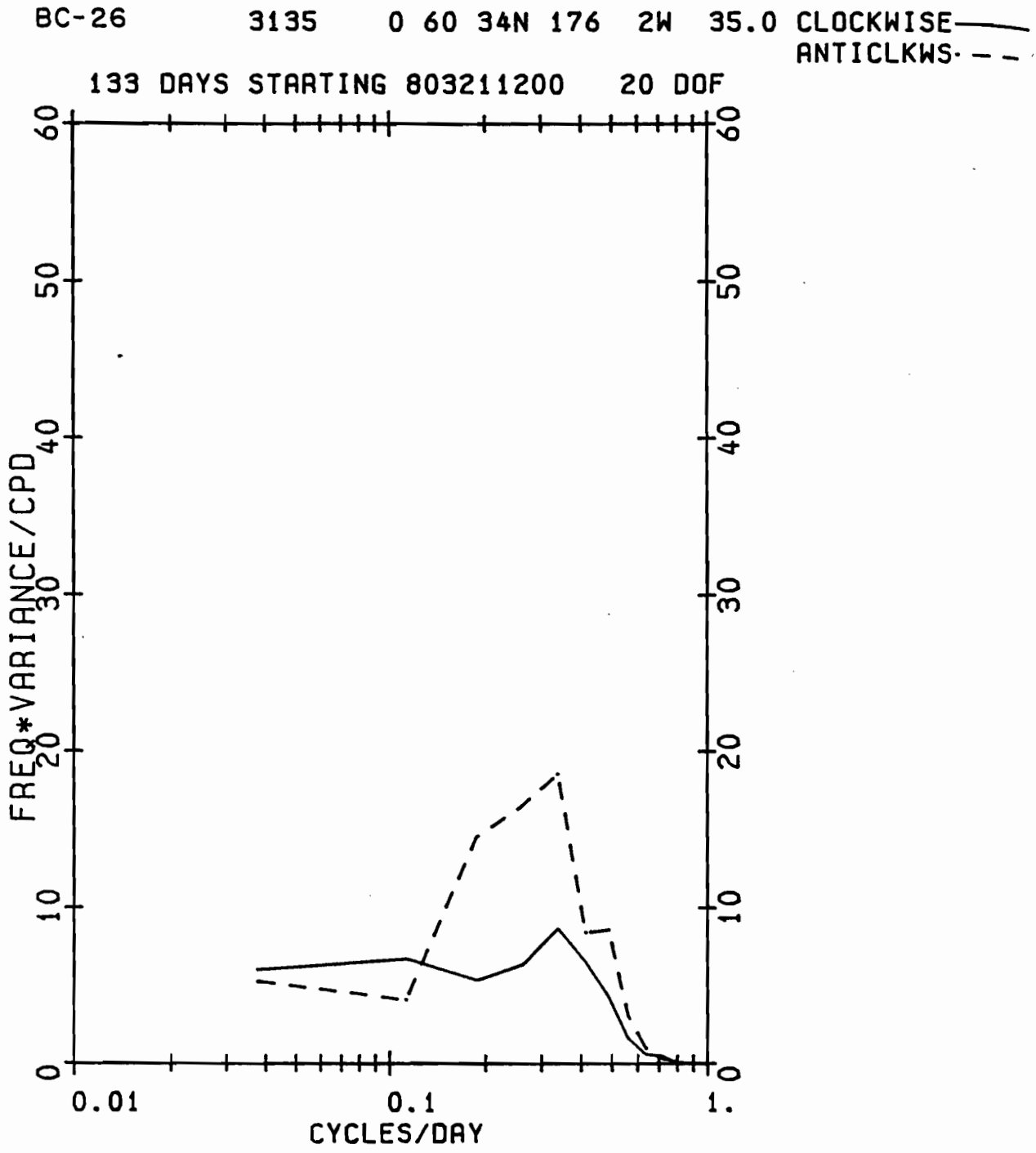


Figure 9g. As in 9f.

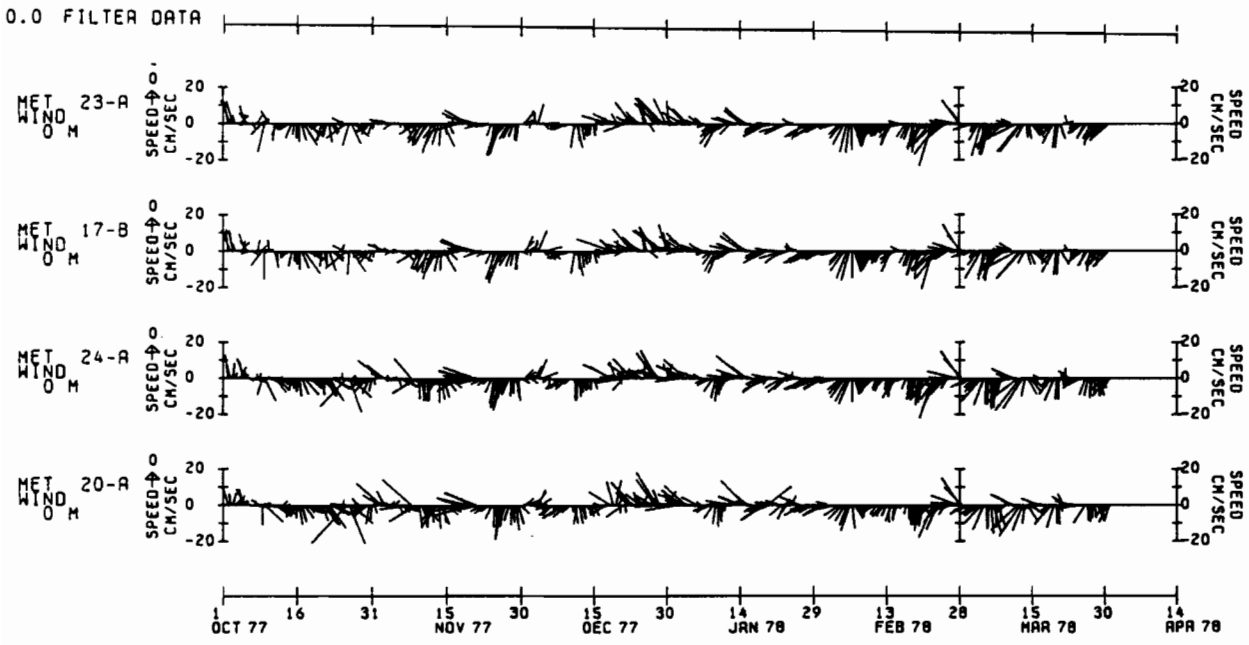


Figure 10. Stick vector representations of the surface winds calculated for the 1977-1978 current meter array.

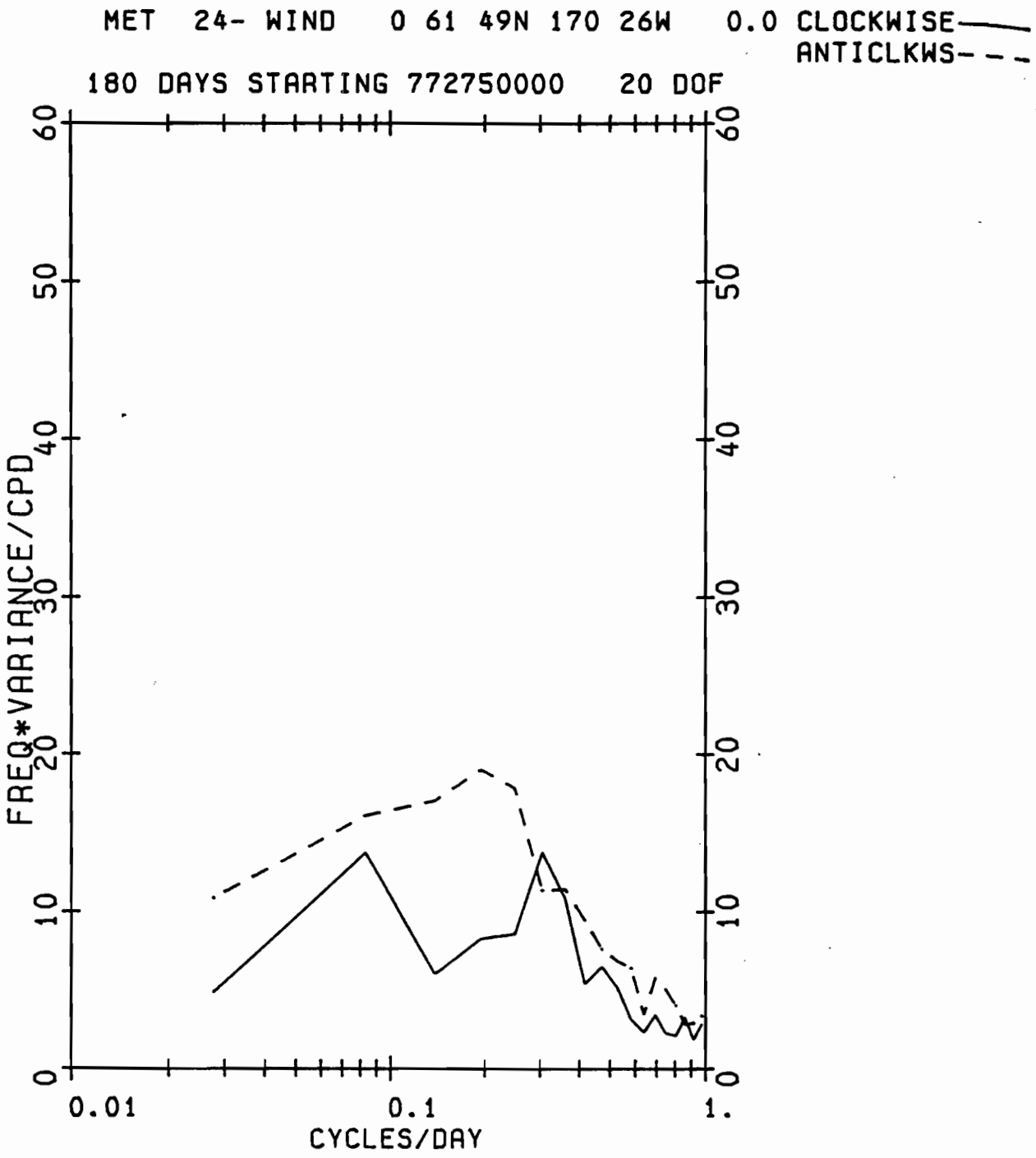


Figure 11a. Rotary spectra of the 1977-1978 surface winds calculated for the same positions as the moorings then in the water. The data interval is 12 hours.

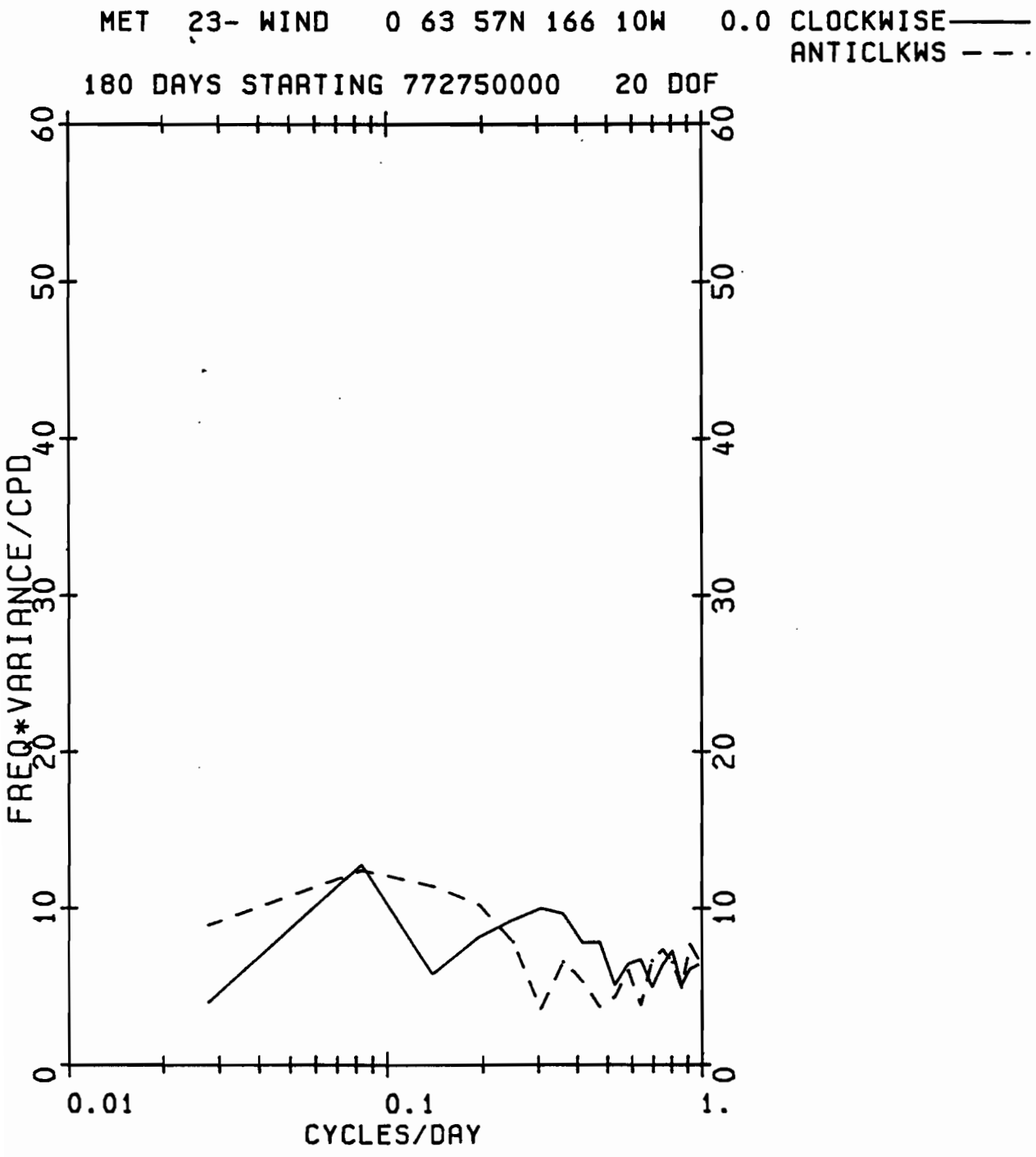


Figure 11b. As in 11a.

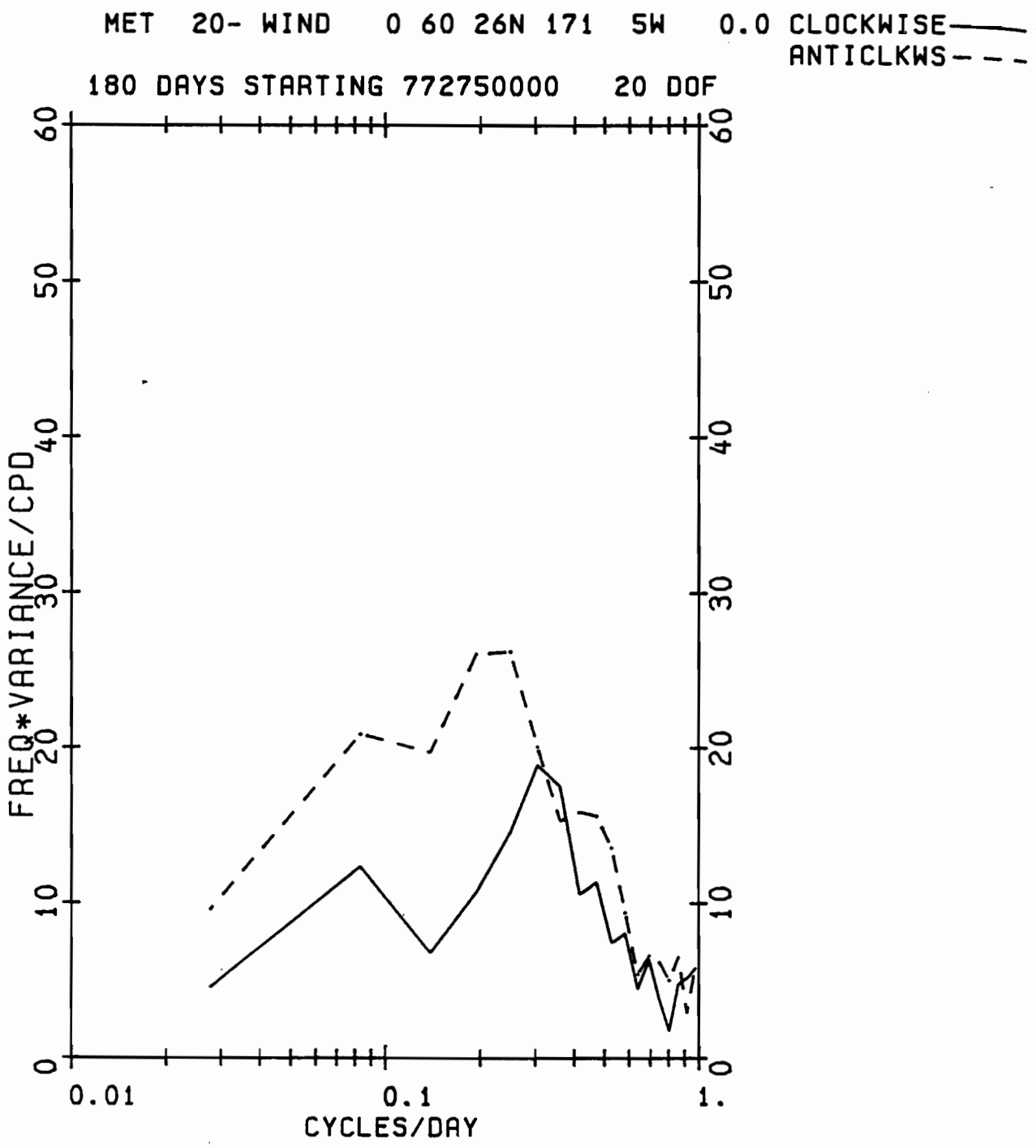


Figure 11c. As in 11a.

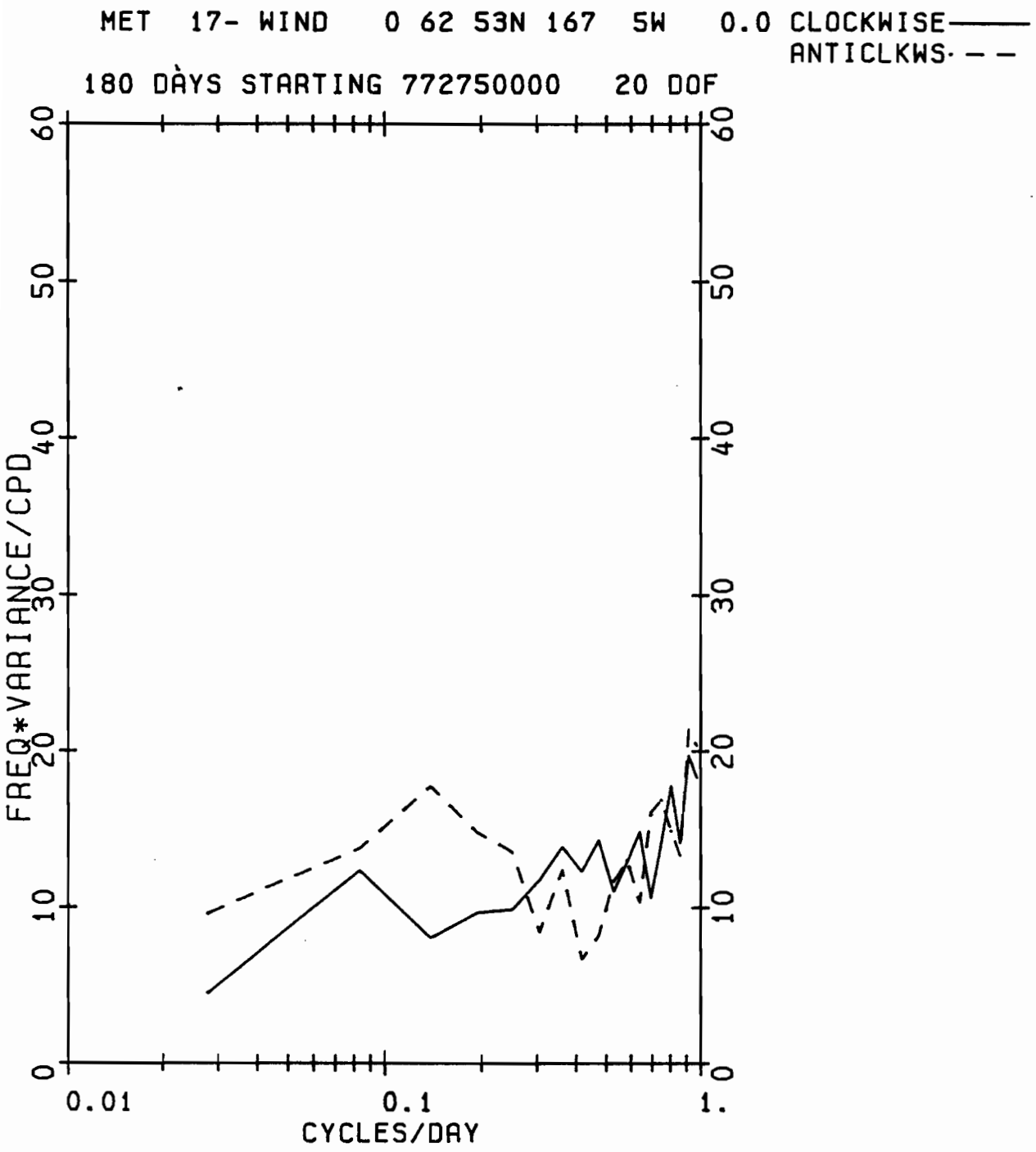


Figure 11d. As in 11a.

Table 5. A comparison of current and wind characteristics for ice-free and ice-covered conditions.

| | Mean Speed | Variance | Vector Mean Speed | Vector Mean Direction (°T) | Axis of Greatest Variance (°T) | Variance on Axis | % Total Var. | Correlation with Wind |
|---|---|---|---|---|---|---|---|---|
| Station | | | | October-November (ice-free) | | | | |
| 24A | | | | | | | | |
| Wind | 9.2 | 20.7 | 3.9 | 194 | 307 | 53.4 | 59.9% | |
| 24m | 10.9 | 89.5 | 4.3 | 003 | 356 | 124.7 | 65.7% | 0.6* |
| 40m | 8.2 | 49.8 | 2.7 | 030 | 346 | 69.9 | 63.2% | 0.5* |
| 20A | | | | | | | | |
| Wind | 9.5 | 23.3 | 3.6 | 189 | 300 | 61.8 | 61.1% | |
| 22m | 7.7 | 39.8 | 4.1 | 314 | 353 | 54.1 | 65.8% | 0.6* |
| 52m | 5.5 | 20.5 | 2.3 | 335 | 358 | 31.3 | 68.4% | 0.5 |
| | | | | January-February (ice-covered) | | | | |
| 24A | | | | | | | | |
| Wind | 10.2 | 15.4 | 8.1 | 240 | 332 | 42.5 | 77.3% | |
| 24m | 7.4 | 17.0 | 4.6 | 007 | 011 | 34.5 | 68.3% | 0.5* |
| 40m | 5.8 | 10.1 | 2.6 | 017 | 359 | 25.7 | 69.6% | 0.4* |
| 20A | | | | | | | | |
| Wind | 9.6 | 16.1 | 6.8 | 244 | 326 | 41.3 | 67.2% | |
| 22m | 7.2 | 20.3 | 5.0 | 342 | 356 | 27.5 | 57.7% | 0.4* |
| 52m | 4.4 | 9.0 | 0.9 | 340 | 324 | 21.5 | 79.0% | --- |

*Where units are cm/s and $cm^2/s^2$ for current speed and variance and m/s and $m^2/s^2$ for wind speed and variance.

# 4. RESULTS

In this Section, current characteristics are discussed, beginning with tidal and proceeding to lower frequency currents. The data were also a differentiated by location: northern records are those from Anadyr and Shpanberg Straits north to Bering Strait, while southern records are those from the open shelf south of St. Lawrence Island.

## 4.1 Tidal Frequencies

While the magnitude of the kinetic energy contained at tidal frequencies was not significantly different in the regions north and south of St. Lawrence Island (except in Bering Strait, NC-10, cf., Figures 4, 9, and Table 4), the percent of the total kinetic energy accounted for by the tides decreased to the north. At sites BC-20A, BC-22, and BC-26, tidal kinetic energy comprised 80% of the total. At the Bering Strait mooring, only 2% of the kinetic energy was due to tides. Moorings located between these two extremes were intermediate in the percent of kinetic energy at tidal frequencies. Tidal kinetic energy was lower at sites in and near Anadyr Strait than in Shpanberg Strait.

On the eastern part of the shelf, the ratio of kinetic energy at diurnal frequencies to that at semidiurnal frequencies generally increased to the north. The ratio was highest at NC-14, where 98% of the tidal kinetic energy was contained at diurnal frequencies, and unlike sites in the eastern strait, semidiurnal tides dominated at these sites, making up 75% of the total.

## 4.2 Wind

Before examining the influence of wind on the measured current, it is necessary to characterize the winds. The total energy at periods greater than 2 days in the METLIB model winds increased to the south when calculated at times and positions matching the 1977-78 current data set. The wind at BC-20A contained nearly 1½ times the kinetic energy of the wind at NC-23. This increase was associated with more energy within the 2- to 10-day band and with the percent of the total energy contained in this band. The spectra suggest that meteorological forcing in the band from 2 to 10 days is only moderately important, since 30-40% of the kinetic energy was contained at periods greater than 10 days. However, the peaks in the spectra did occur within the 2- to 10-day limits.

There was 2-3 times as much energy in the anticlockwise component of spectra at the southern sites than at the northern sites. This increase is undoubtedly caused by the greater number of cyclonic low-pressure centers which traverse the southern Bering Sea, whose effects are manifested more strongly at the southern sites. The amplitude of the clockwise component at periods of 3-5 days at BC-20A is nearly double that at NC-23A, and this may reflect the impact of the other primary storm track which carves northward from the Aleutian Islands toward Siberia (Overland and Pease, 1982).

The mean speeds of the METLIB winds increase from the lowest value of 8.9 m/s at NC-23A, in the north, to the highest value of 9.8 m/s at BC-20A, the southernmost mooring. Variance of the mean speed did not show a similar pattern, although it was markedly greater at St. Paul Island farther to the south.

The magnitude of the vector-mean wind decreased to the south, from 5.4 m/s at NC-23A to 4.5 m/s at BC-20A. The direction of the vector-mean wind was toward the southwest and varied little over the region. The principal axis of the wind veered 30° from the northernmost to the southernmost site, with little change in the percent of the energy along that axis.

## 4.3 Meteorological Forcing

Current energy contained within the 2- to 10-day band of 35-hr rotary spectra increased nearly monotonically from south to north, as did the ratio of energy at these frequencies to the total energy (Fig. 9). Within this spectral band, usually attributed to meteorological forcing, currents at most northern sites contained a peak at approximately ten days. In 1976-1977 this peak was present in both the clockwise and anticlockwise components in the record from Bering Strait but absent from records in Shpanberg Strait; records from the latter moorings did have a prominent peak at about 5 days. In 1977-1978 the two records from north of St. Lawrence contained a peak at 10 days which was stronger in the anticlockwise component. This peak was absent in records from the open shelf. In 1980-1981, the 10-day peak was most evident in the record from NC-19B, and as a shoulder on a 5-day peak in the record from NC-26A. In both cases, the clockwise component dominated. The 10-day peak was absent at the other sites except as a small, broad feature at BC-26.

The incidence of southerly flow events in Shpanberg Strait identifies the 1976-1977 5-day peak and the 1977-1978 and 1980-1981 10-day peak with these reversals (see Figure 3). Both a 10-day and 5-day peak appeared at NC-10 in Bering Strait. There were 16 distinct episodes of southerly flow at that site within the 180-day analysis period, and these correspond to the 10-day peak. The 5-day peak may reflect modulation of the currents by the reversals occurring upstream at NC-16 and NC-17A.

It was more difficult to determine the number of southerly flow events which occurred on the southern shelf, because of the reduced preference of flow direction. Between 15 and 25 southerly flow events occurred in the 180-day analysis period at moorings to the south, which would be in accord with peaks at 7-10 days. Only NC-24A and NC-26, near the St. Lawrence Island channels, contained peaks at 10 days, although all moorings contained a peak at 5 days. The dominant peak at a southern site was usually near either 2.8 or 3.5 days. In 1977-1978 there was a peak in the clockwise component at 2.8 days at both NC-24A and BC-20A, though this peak was dominated by an anticlockwise peak at about 3.7 days at BC-20A. The 2.8-day feature was also manifest at the northern moorings, but in the anticlockwise component. In 1980-1981, only the southernmost site had a 2.8-day peak; the major peak at BC-22 was at 3.5 days in the anticlockwise component.

## 4.4 Mean Currents

Mean current speed and the variance of mean speed both increased to the north in 1977/78 and 1980/81. The mean speed in the straits east and west of St. Lawrence Island was two-to-three times that observed near St. Matthew Island. This trend continued north of St. Lawrence Island; in 1976/77 the mean speed in Bering Strait was nearly twice that observed in Shpanberg Strait. Although some of the increase was likely due to constriction of flow north of St. Lawrence Island, except in 1976/1977 the northern meters tended to be in shoaler water which also contributed to the observed variation. Further, it is not known how representative the measurements at one site are of the flow field across the entire strait. There is a suggestion of lateral shear in Anadyr and Shpanberg Straits and observations of such north of Bering Strait (Coachman and Aagaard, 1981).

The magnitude of the vector-mean current also increased to the north, and all but two sites had a northward vector mean. At most sites the direction of the vector-mean flow was within 15° of the trend of the isobaths, as was the axis of greatest variance. The percent of variance along this axis differed markedly between northern and southern moorings. At sites north of St. Lawrence Island, more than 90% of the variance occurred on the principal axis. Except at BC-22 on the open shelf and NC-25A, very near St. Lawrence Island, all of the open-shelf records contained less than two-thirds of the total record variance on this axis. This difference is also obvious in the current roses (Figure 5). Current roses at the southern sites are more isotropic; currents in the north have a strongly preferred direction along bathymetry.

In Shpanberg Strait, the magnitude and direction of the vector-mean current is primarily a function of the number and strength of reversals which occur during a given period. During 1976/77, 22 reversals occurred at NC-17A and NC-16 in the 180-day period of analysis, with the longest event lasting about two weeks. There were only 14 reversals in the same period at NC-17B (1977/78). The impact of reversals was such that the net current at NC-17A was 4.4 cm/s at 354° at NC-17B. Some of the difference between net current at NC-16 and NC-17A may be a result of weaker reversals (particularly during fall) at NC-16. This suggests more persistent northward flow in the eastern part of Shpanberg Strait and also, as noted above, lateral shear across the strait.

At mooring NC-19B in Anadyr Strait, there were nine reversals during the 136 days of the analysis, but the reversals were mostly weak and of short duration (Fig. 3C). Currents were more steadily northward, with variations in speed at roughly ten-day periods obvious in the record. Because of the weaker reversals, the magnitude of the net current was significantly greater at NC-19B than at any of the other sites in the eastern channel, although the mean speed at NC-19B was different only from NC-17B at a 95% level of significance.

In both 1976/77 and 1977/78, current reversals were stronger and more frequent in the autumn; and there was a period without significant reversals from mid-December through most of January. In Anadyr Strait, this period occurred in November and December. Reversals in Shpanberg Strait ceased at

approximately the same time that the moorings became ice-covered; however, Anadyr Strait was not ice-covered until mid-December. Further, ice-cover persisted through January at all sites. While ice-cover cannot be the only reason reversals cease, it may be a related factor.

## 4.5 Time-Series Comparisons

The highest correlations were for the flow between closely spaced sites in the region north of St. Lawrence Island, where the correlation coefficients were greater than 0.8 (Table 3). On the open shelf, the value of the correlation coefficient varied from 0.67 for NC-24A compared to BC-20 to 0.12 (below the 95% level) for BC-22 and BC-26. It is interesting that flow at the northern mooring NC-19B was better correlated with flow at NC-25, south of St. Lawrence Island, than with NC-26, which was closer and near the Gulf of Anadyr. Schumacher et al. (1983) suggest that currents at both NC-19B and NC-25 are part of the regional circulation, whereas NC-26 is south of the flow, hence the observed pattern of correlations.

For comparisons in which the correlation increased at a lag of six hours, the correlation was usually better for the case of the southern mooring leading the northern one. This is in agreement with the fact that the vector-mean current was usually directed to the north. Some comparisons involving BC-19B and NC-26 counter this finding, although two of the four comparisons involved were not significantly correlated.

Vertical correlations at sites NC-24A and BC-20A were high ($\sim$0.9). Currents were in phase NC-24A, but at BC-20A the correlation was enhanced for the bottom meter leading the surface meter by six hours.

The spatial pattern of coherence was similar to that of correlation (Fig. 12). Closely spaced northern sites, such as NC-17A with NC-16 and NC-23 with NC-17B, were coherent at all frequencies. As the distance between moorings increased or the difference in depths became greater, the level of coherence decreased. Coherence, like correlation, was generally lower for a comparison of two open-shelf moorings.

The frequency at which the major peaks of the coherence spectra occurred was quite variable. Graphs involving two northern meters which had strong signals in their rotary spectra arising from reversals were strongly coherent at the common frequency of the reversals. An example of this is the peak at 5 days in the NC-17A and NC-16 comparison. Although NC-17A did not contain a peak at ten days, it is coherent with NC-10 at that period, since the peak at five days was a harmonic of the ten-day peak. Almost all graphs, not just those north of St. Lawrence, contained a peak at five days, although not all the peaks were significant. Nearly all data were coherent at periods greater than ten days, although there was not always a peak in this region.

A feature common to all comparisons was a decrease in coherence at periods ranging from seven to ten days. In some cases, coherence at this period was nearly zero. This decrease occurred even in the two vertical coherences, although the comparisons remained coherent at all

frequencies. Currents at each of the four 1977/78 moorings were correlated to the local wind at above the 95% confidence level. Flow at NC-17B was better correlated to winds at NC-23 and at NC-24A than to local winds, perhaps due to the funneling of wind-driven flow from either end of the channel. Correlation improved for all comparisons when the currents lagged the winds by 12 hours.

The major peak in the coherences of the winds and currents was centered at roughly ten days. Only the comparison at NC-23A contained a second peak, near three days. The ten-day period corresponds well to the ten-day peak ascribed to southerly flow events at NC-23A and NC-17B. It is somewhat puzzling that the only peak at NC-24A and NC-17B was at ten days, since the currents and winds at both sites contained more energy at five days.

## 4.6 Currents and Winds During Ice-covered Versus Ice-free Conditions

The mean speed of the currents decreased at both depths at NC-24A (32% at the upper level vs. 29% at the lower level) and BC-20A (7% at the upper level vs. 20% at the lower level) when the mooring sites were ice-covered, although the mean speed of the wind increased slightly. Kinder and Schumacher (1981) noted similar decreases in mean speed when moorings were ice-covered and attribute some of the decrease to reduced surface-wave action and hence less rotor pumping. However, accompanying the reduction of current speed was a change in phase of the tide (Pearson et al., 1981). While it is clear that ice cover affects the currents, their mode of interaction is uncertain.

During the period of ice-cover in January-February, the vector-mean speed of the wind was about double its value in October-November. The direction of the vector-mean wind rotated clockwise from nearly due south to southwest. The principal axis also rotated clockwise, and the percent of variance occurring on the axis increased.

The vector-mean speed of both upper-current records increased during the January-February period, although vector-mean speed decreased at the lower meters. Like the vector-mean wind, the direction of the vector-mean current, and the principal axis of variance rotated clockwise. The resultant direction in each case was closer to a hypothetical line connecting the mooring to Shpanberg Strait.

Currents and wind were correlated at greater than the 95% level for both the ice-free and ice-covered time periods. However, the correlation coefficient decreased for the ice-covered case, with a greater decrease at the lower meter than at the top. Although correlation in October-November was enhanced for one lag, with winds leading currents, there was no such increase in correlation in January-February.

Because of the decrease in correlation coefficient, the increase in the vector-mean current magnitude without an accompanying increase in the mean speed, and the rotation of the currents towards Shpanberg

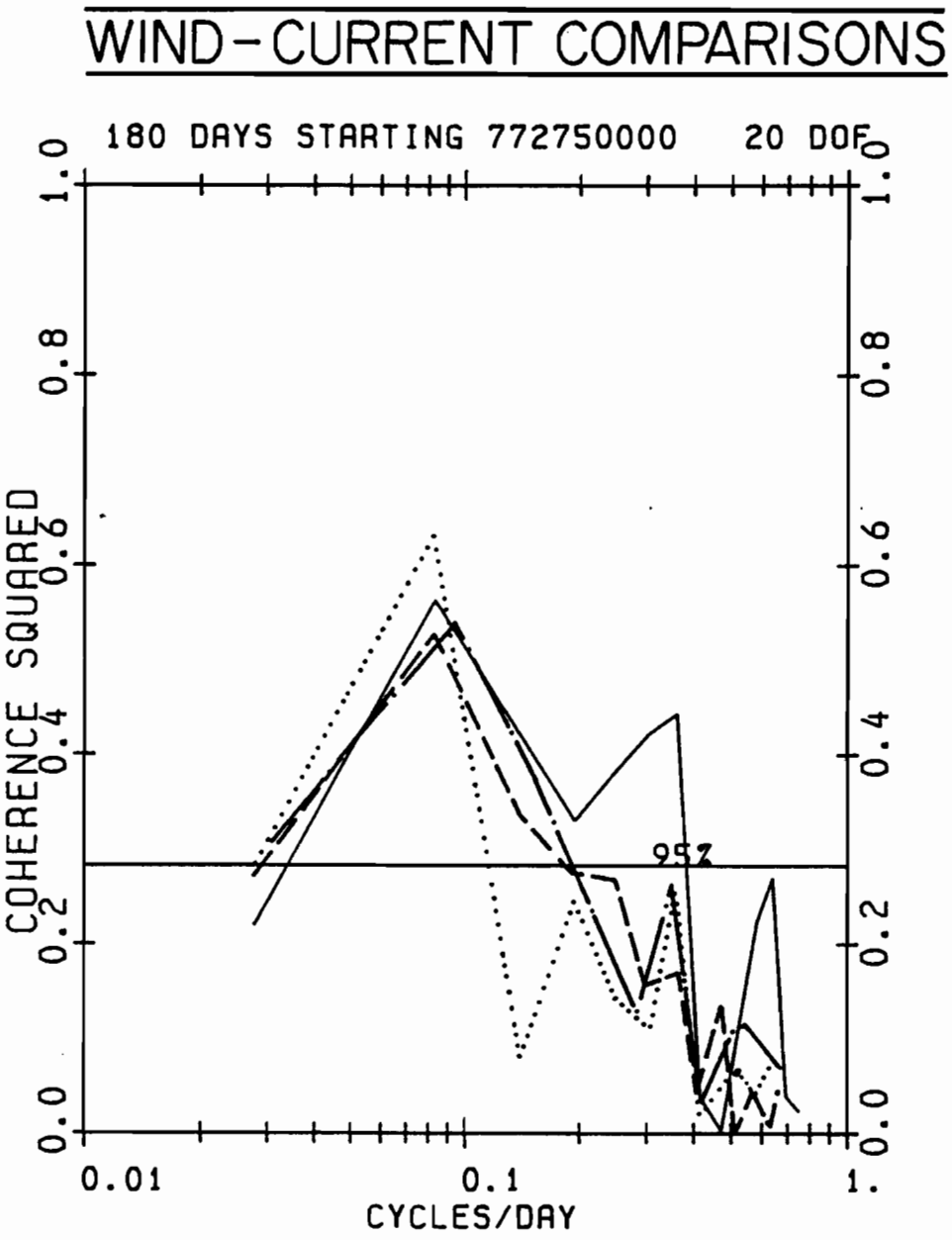


Figure 12. Coherence of the 1977-78 currents with the surface winds calculated for each site. The surface meter was used at moorings NC-24A and BC-20A.

——— NC-23A
– – – – NC-17B
. . . . NC-24A
– . – . BC-20A

Strait during the ice-covered period, we conclude that the ice acted to alter the usual impact of wind stress. This interaction allowed currents to respond more freely to the mean driving forces for northward flow. The decrease in the magnitude of the vector-mean flow at the lower meters cannot be directly explained by diminished wind stress, since the vector-mean speed at the upper meters increased. Perhaps interactions with bathymetry, resulting from changes in direction, were involved.

## 5. DISCUSSION

Clear characteristics contained in the current records are: 1) an increase of kinetic energy to the north in the meteorological, low-frequency and mean bands, and a consequent increase in the ratio of kinetic energy in these bands to the total kinetic energy of fluctuations, 2) a decrease of the percent of the tidal to total kinetic energy of fluctuations to the north, although there was less variation in the magnitude of kinetic energy of the tides themselves, and 3) in Anadyr Strait stronger vector-mean flow and kinetic energy of this mean, but lower values of kinetic energy within the other frequency bands than in Shpanberg Strait. However, because simultaneous measurements were not obtained, the latter characteristic may be a manifestation of interannual current variation.

The first two characteristics suggest that the present study area of the eastern Bering Sea shelf may be considered as two regions: the open shelf south of St. Lawrence Island and the more constricted area north of St. Lawrence, including the two straits on either side.

Kinetic energy in the southern region (except at NC-26A and NC-25A) was dominated by tides which accounted for as much as 80% of the total kinetic energy. Tides were predominantly semidiurnal. Mean current speeds were typically 5 to 10 cm/s and the vector-mean speed was less than 4 cm/s. The direction of the current was generally toward the north, except when local bathymetry tended E-W where flow was generally close to the direction of the isobaths. Only 55-65% of the variance of the vector-mean current occurred on the principal axis, which also agreed well with the alignment of local isobaths.

Currents were significantly correlated, except for comparisons involving either the near-shore mooring (NC-14) or records from greatly different depths or positions. For similar separations, correlation coefficients north of St. Lawrence were comparable to those seen on the open shelf; NC-10 to NC-17A and NC-23A to NC-24A both have a correlation of 0.5. Almost all correlation coefficients were enhanced in a lagged correlation in which the northern station lagged the southern one by six hours (one data point). Coherency spectra contained strong peaks at frequencies which can be identified with the frequency of reversals, notably at five and ten days. Currents north of St. Lawrence Island were better correlated to the local METLIB winds than were the currents on the open shelf. The major peak in their coherence was at ten days.

Kinder and Schumacher (1981) described three flow regimes as a function of depth on the southeastern Bering Sea shelf. In the coastal regime, shallower than 50 m, greater than 90% of the fluctuating kinetic energy was tidal, vector-mean flow was 1-5 cm/s, and wind events were visible in the data records. Tides accounted for about 90% of the fluctuating kinetic energy in the middle regime, between 50-100 m depth, where vector-mean speeds were 0.5 cm/s except near 50 m, where they were 2-5 cm/s. Again, wind events were obvious in the data. They were not visible in the outer regime, deeper than 100 m, where the kinetic energy was about 80% tidal and vector-mean flow was of 1-5 cm/s. The southern shelf meters of the present data set fit their classification scheme well. Meters north of St. Lawrence Island do not agree with their categories because of the greatly increased mean flow. Due to the small size of the data set, the possibility of similar depth-related regimes north of St. Lawrence Island cannot be examined.

In the region north of St. Lawrence Island, from 2-36% of the total kinetic energy was accounted for by tides. The decrease in the relative importance of the tides was due primarily to an increase of the energy at meteorological and low-frequency periods. North of St. Lawrence Island, tides were predominantly diurnal, except in Anadyr Strait. Mean-current speeds were greater than 15 cm/s; vector-mean speeds were from 4-15 cm/s. The magnitude and direction of the vector-mean current appear to have been controlled by the number and magnitude of current reversals which occurred at the site; this is particularly evident at NC-17A in 1976. Greater than 90% of the variance of the vector-mean current occurred on the principal axis, whose direction was near that of the local bathymetry.

In summary, flow in the region north of St. Lawrence Island was strongly directional as a result of an increase in the magnitude of the vector-mean current. Currents in the region were horizontally coherent and well correlated, and the mean flow accounted for a large proportion of the total fluctuating kinetic energy. Although currents on the open shelf were well correlated and coherent, the flow did not have a strongly preferred direction; nor was the mean flow responsible for a large part of the fluctuating kinetic energy. The effect of the organized current which would appear to be operating in the region north of St. Lawrence Island is felt on the open shelf, however, in the northerly direction of the vector-mean flow. This effect of the current is easily seen in the rotation of the vector-mean current direction at NC-24A toward the eastern St. Lawrence Strait.

To delineate the differences between the two regions, the average values of fluctuating kinetic energy contained within tidal, meteorological, and low-frequency bands within the two regions were tabulated (Table 5, bottom). The similarity in the magnitude of tidal energy in the two areas is evident. The most striking result is the ten-fold increase in the energy contained at meteorological and low-frequency components of flow.

Ice in the strong northerly currents of the northern Bering Sea requires strong northerly winds to be advected south. Northerly winds are common in winter and instances of southerly advection of ice are numerous (Muench and Ahlnäs, 1976; McNutt, 1980). However, under more quiescent conditions or southerly winds, ice motion to the northwest has also been noted (Pease and Salo, 1981). At all times, currents are more important in determining ice drift in the northern region than the open shelf, with its weaker total kinetic energy and relatively weak mean flow.

Ice cover on the southern shelf may allow the flows of the northern region to exert a greater influence on open-shelf currents by decreasing the transmission of wind stress associated with the predominantly northerly winds. Thus, vector-mean flows were of greater magnitude during ice-covered periods. An unresolved problem in this regard is the resumption of flow reversals during January, a time when the ice cover is extensive over the open shelf.

## 6. SUMMARY

This report draws upon the records of fifteen moored current meters to delineate characteristics of currents on the Bering Sea shelf in winter. The data set does not provide adequate spatial or temporal coverage to allow an exhaustive description of the flow patterns. However, it can be seen that the study area is divided by geography and by current characteristics into the constricted region north of St. Lawrence Island and the open shelf to the south of the island.

Currents in the northern region were dominated by mean flow and currents at meteorological and low frequencies. Kinetic energy at tidal frequencies comprised 30-35% of the total fluctuating kinetic energy near St. Lawrence Island, and only 2% of the total at Bering Strait. In contrast, up to 85% of the total fluctuating kinetic energy occurred at tidal frequencies on the open shelf, and as little as 11% was at low frequencies.

The vector-mean current was in general northward and paralleled the local trend in bathymetry nearly everywhere. In the north, the principal axis was strongly preferred, while flow on the open shelf was less directionally stable. This can be regarded as a consequence both of the proximity of the northern meters to the Bering Strait flow field and to the constriction of flow by geography in the region.

On the northern shelf, current reversals were responsible for a spectral peak generally at 5 or 10 days. Although reversals occurred on the open-shelf with a frequency in accord with a 7- to 10-day peak, this peak was usually not present in the spectra, possibly because of the inherently greater heterogeneity in current direction.

Correlation and coherence were significant for both regions and for interregional comparisons. For 1977-1978 when METLIB wind fields were available, currents were also well correlated and coherent with the local winds.

The northerly currents are obviously important in modifying the advection of ice, especially in the northern region. As the northern region is thought to be the formation area of much of the Bering Sea ice, further examination of the interactions among wind, ice, and currents in this region is necessary. In addition, it is possible that the presence of ice on the open shelf may allow the northward Bering Strait flow to be felt more strongly on the open shelf.

## 7. Acknowledgements

This memorandum is a contribution to the Marine Services Project of NOAA's Pacific Marine Environmental Laboratory. Data were made available for this study by K. Aagaard, R. B. Tripp, R. D. Muench, and the Marine Meteorological Studies Group of PMEL. C. H. Pease reviewed the manuscript.

This study was funded in part by the Bureau of Land Management through an interagency agreement with the National Oceanic and Atmospheric Administration, under which a multiyear program is being conducted to respond to the need for petroleum development on the Alaskan Continental Shelf, and is managed by the Outer Continental Shelf Environmental Assessment Program (OCSEAP).

## 6. REFERENCES


Coachman, L.K. and K. Aagaard (1981): Reevaluation of water transports in the vicinity of Bering Strait, in The Eastern Bering Sea Shelf: Oceanography and Resources, Volume 1 (ed. by D.W. Hood and J.A. Calder), Government Printing Office (dist. by University of Washington Press, Seattle), 77-94.

Coachman, L.K., K. Aagaard, R.B. Tripp (1975): Bering Strait, The Regional Physical Oceanography, University of Washington Press, Seattle, 172 pp.

Kinder, T.H. and J.D. Schumacher (1981): Circulation over the continental shelf of the southeastern Bering Sea, in The Eastern Bering Sea Shelf: Oceanography and Resources, Volume 1, (ed. by D.W. Hood and J.A. Calder), Government Printing Office (dist. by University of Washington Press, Seattle), 31-52.

Newton, J.L. and B.G. Anderson (1980): MIZPAC 80A USCGC Polar Star (WAGB-10) Arctic West Operations March 1980: Bering Sea Cruise Report and Preliminary Oceanographic Results, SAI202-80-460-LJ, Science Applications Inc., La Jolla, CA, 38 pp.

Muench, R.D. (1983): Mesoscale oceanographic features associated with the central Bering Sea ice edge: February - March 1981, J. Geophys. Res., 88, 2715-2722.

Muench, R.D., R.B. Tripp, and J.D. Cline (1981): Circulation and hydrography of Norton Sound, in The Eastern Bering Sea Shelf: Oceanography and Resources, Volume 1 (ed. by D.W. Hood and J.A. Calder), Government Printing Office (dist. by University of Washington Press, Seattle), 77-93.

Overland, J.E. (1981): Marine climatology of the Bering Sea, in The Eastern Bering Sea Shelf: Oceanography and Resources, Volume 1 (ed. by D.W. Hood and J.A. Calder), Government Printing Office (dist. by University of Washington Press, Seattle), 15-22.

Overland, J.E., R.A. Brown, and C.D. Mobley (1980): METLIB - A Program Library for Calculating and Plotting Marine Boundary Layer Wind Fields, NOAA Technical Memorandum, ERL PMEL-20, 82 pp.

Overland, J.E. and C.H. Pease (1982): Cyclone climatology of the Bering Sea and its relation to sea ice extent, Monthly Weather Review, 110, 5-13.

Pease, C.H. (1980): Bering Sea ice processes, Monthly Weather Review, 108, 2015-2023.

Pease, C.H., S.A. Schoenberg, and J.E. Overland (1982): A Climatology of the Bering Sea and its Relation to Sea Ice Extent, NOAA Technical Report, ERL 419-PMEL 36, 29 pp.

Pearson, C.A. (1981): Guide to R2D2 - Rapid Retrieval Data Display, NOAA Technical Memorandum, ERL PMEL-29, 148 pp.

Pearson, C.A., H.O. Mofjeld, and R.B. Tripp (1981): Tides of the eastern Bering Sea shelf, in The Eastern Bering Sea Shelf, Oceanography and Resources, Volume 1, (ed. by D.W. Hood and J.A. Calder) Government Printing Office (dist. by University of Washington Press, Seattle), 53-85.

Salo, S.A., C.H. Pease, and R.W. Lindsay (1980): Physical Environment of the Eastern Bering Sea, March 1979, NOAA Technical Memorandum, ERL PMEL-21, 119 pp.

Schumacher, J.D., K. Aagaard, C.H. Pease, and R.B. Tripp (1983): Effects of a shelf polynya on flow and water properties in the northern Bering Sea. J. Geophys. Res., 88, 2723-2733.

Takenouti, A.Y. and K. Ohtani (1974): Currents and water masses in Bering Sea: A review of Japanese work, in Oceanography of the Bering Sea with Emphasis on Renewable Resources (ed. by D.W. Hood and E.J. Kelley), Institute of Marine Science, University of Alaska, Fairbanks, 39-58.

Webster, B.D. (1981): A Climatology of of the Ice Extent in the Bering Sea, NOAA Technical Memorandum, NWS AR-33, 38 pp.